International Journal of *Molecular Sciences*

MDPI

Article

The conservation of m^{6}A methyltransferase (METTL) genes and loss of functions caused development arrest in *G. hirsutum*

Junfeng Cao[1,2,3], Chaochen Huang[2], June Liu[4], Chenyi Li[2], Xia Liu[5], Zishou Zheng[2], Lipan Hou[2], Jinquan Huang[2], Lingjian Wang[2], Yugao Zhang[5], Xiaoxia Shangguan[2,6*], Zhiwen Chen[1,2*]

[1] Hainan Yazhou Bay Seed Laboratory, Sanya 572025, China; chenzw@yazhoulab.com (Z.C.)
[2] National Key Laboratory of Plant Molecular Genetics and National Center for Plant Gene Research, Institute of Plant Physiology and Ecology/CAS Center for Excellence in Molecular Plant Sciences, Chinese Academy of Sciences, Shanghai 200032, China; caojunfeng@sibs.ac.cn (J.C.); jane525265016@sina.com (C.H.); Chyli@cemps.ac.cn (C.L.); zhengzishou@sippe.ac.cn (Z.Z.); houlipan@cemps.ac.cn (L.H.); huangjinquan@sibs.ac.cn (J.H.); ljwang@sibs.ac.cn (L.W.); sgxx74@126.com (X.SG.)
[3] Key Laboratory of Urban Agriculture (South), Ministry of Agriculture, Plant Biotechnology Research Center, Fudan-SJTU-Nottingham Plant Biotechnology R&D Center, School of Agriculture and Biology, Shanghai Jiao Tong University, Shanghai 200240, China; caojunfeng@sibs.ac.cn (J.C.)
[4] School of Life Sciences, Peking University, Beijing 100871, China; liujune@pku.edu.cn (J.L.)
[5] Esquel Group, 25 Harbour Road, Wanchai, Hong Kong, China; liuxiaxj@esquel.com (X.L.); zhangyu@esquel.com (Y.Z.)
[6] Institute of Cotton Research, Shanxi Agricultural University, Yuncheng 044099, China
* Correspondence: sgxx74@126.com (X.SG.); chenzw@yazhoulab.com (Z.C.)

Abstract: N6-methyladenosine (m^{6}A) RNA modification plays important regulatory roles in crop development and adapting to the environment, which requires methyltransferases to achieve the methylation process. However, there has been no research regarding m^{6}A RNA methyltransferases in cotton. Here, a systematic analysis of the m^{6}A methyltransferase (METTL) gene family was performed on twelve cotton species, resulting in six METTLs identified in five allotetraploid cottons, respectively, and three to four METTLs in the seven diploid species. Phylogenetic analysis of protein-coding sequences revealed that *METTL* genes from cottons, *Arabidopsis thaliana* and *Homo sapiens* could be classified into three clades (METTL3, METTL14 and METTL-like clades). *Cis*-element analysis predicated the possible functions of *METTL* genes in *G. hirsutum*. RNA-seq data revealed that *GhMETTL14* (*GH_A07G0817*/*GH_D07G0819*) and *GhMETTL3* (*GH_A12G2586*/*GH_D12G2605*) had high expressions in root, stem, leaf, torus, petal, stamen, pistil and calycle tissues. *GhMETTL14* also had the highest expression in 20 and 25 dpa fiber cells, implying a potential role at the cell wall thickening stage. Suppressing *GhMETTL3* and *GhMETTL14* by VIGS caused development arrest and even to death in *G. hirsutum* along with the decreased m^{6}A abundance from the leaf tissues of VIGS plants. Overexpression of *GhMETTL3* and *GhMETTL14* produced distinct differentially expressed genes (DEGs) in *A. thaliana*, indicating their possible divergent functions after gene duplication. Overall, GhMETTLs play indispensable but divergent roles during the growth of cotton plants, which provided the basis for the systematic investigation of m^{6}A in the subsequent study to improve the agronomic traits in cotton.

Keywords: m^{6}A methyltransferase; Cotton; Phylogenetics; VIGS; divergent function

Citation: Cao, J.; Huang, C.; Liu, J.; Li, C.; Liu, X.; Zheng, Z.; Hou, L.; Huang, J.; Wang, L.; Zhang, Y.; Shangguan, X.; Chen, Z. *Int. J. Mol. Sci.* **2022**, *23*, x.

Academic Editor:

Received: date
Accepted: date
Published: date

1. Introduction

N6-methyladenosine (m^{6}A) methylation is the most abundant post-transcriptional modification of RNAs in mRNA [1, 2]. m^{6}A RNA methylation is a dynamic process and highly conserved in mammals, flies and plants, which is mediated by m^{6}A writer, eraser, and reader proteins [3]. The m^{6}A methylation writer complex is composed of the m^{6}A methyltransferases and other factors, e.g., WTAP. METTL3 was the first m^{6}A RNA

methyltransferase identified in *Homo sapiens* [4]. Subsequently, METTL14 was identified as the second m^{6}A methyltransferase in humans with high homology to METTL3 [5, 6]. Actually, subsequent studies showed that METTL14 had no methyltransferase activity but could bind to RNA substrates by interacting with METTL3 to form a heterodimer [7-9]. WTAP was also a major binding partner of the complex [10]. WTAP interacted with METTL3 and METTL14, and was required for the METTL3-METTL14 heterodimer localization into nucleus for the catalytic activity of the m^{6}A methyltransferase complex [10].

Recently, researches on m^{6}A writers have also been conducted in plants extensively, including the m^{6}A methyltransferase components being characterized in *Arabidopsis*. For example, AtMTA (METTL3 human homolog protein) was one of the earliest discovered m^{6}A methyltransferases in *Arabidopsis* [11]. AtMTA proteins were actively distributed in the reproduction organs and apical meristems of *Arabidopsis* plants. AtMTA protein was required for the m^{6}A mRNA methylation, and its function disruption prevented plant embryos development, further resulted in embryo lethality [11]. In addition, PtrMTA, a *Populus trichocarpa* methyltransferase MTA homologous protein, was colocalized in the nucleus. PtrMTA-overexpressing plants significantly enhanced the tolerance to drought stress by increasing the density of trichomes and roots in poplar [12]. AtMTB was the human METTL14 homologous protein identified in *Arabidopsis*, but its function was unknown [13]. However, ClMTB, an AtMTB homolog protein in watermelon and its expression was induced under drought stress. Overexpression of *ClMTB* enhanced drought tolerance by elevating the reactive oxygen species (ROS) scavenging ability and alleviating photosynthesis inhibition in tobacco [14]. Both these MTAs and MTBs belong to the MT-A70-like (MT) proteins [3]. These results implied that the m^{6}A methyltransferases might serve as the positive regulatory factors in response to the different adverse stresses.

As the m^{6}A methyltransferases were highly conserved, thus, the protein methyltransferases in H. sapiens and *Arabidopsis* would provide the necessary sequence references to identify the orthologous proteins or genes in other different plant species. Cotton (*Gossypium* genus) is the most important fiber crop worldwide and this genus contains more than 50 species [15-18]. As much *Gossypium* plant genome information was publicly available, such as diploid D sub-genome species, *Gossypium thurberi* (D1), *G. raimondii* (D5), G. turneri (D10) [19-22], diploid A sub-genome species *G. herbaceum* (A_1), *G. arboreum* (A_2) [23-25], diploid F sub-genome specie *G. longicalyx* (F_1) [26], diploid G sub-genome specie *G. australe* (G) [27] and allotetraploid species *G. hirsutum* (AD_1), *G. barbadense* (AD_2), *G. tomentosum* (AD_3), *G. mustelinum* (AD_4) and *G. darwinii* (AD_5) [25, 28-35], as well as *Gossypium* sister genera *Gossypioides kirkii* [36]. These genome sequences will provide a good platform for performing the comparative genomics analysis and dissecting their gene functions. As the m^{6}A methyltransferases (METTL) genes in *Gossypium* have not been investigated, some representative *Gossypium* species were selected to characterize the m^{6}A methyltransferase genes and their roles in cotton.

In this study, we performed a genome-wide screening for METTL genes in cottons, based on data gathered from recent whole-genome sequencing results. We used in silico approach to identify and characterize METTL genes, and then focused on the characterization and phylogenetic relationships of *Gossypium* species. The METTL gene structures, conserved domains, as well as cis-elements were explored in this systematical analysis. Moreover, the tissue-specific expression patterns and the transcriptional responses of GhMETTLs to abiotic stresses were examined. The possible biological functions of *GhMETTL3* and *GhMETTL14* were investigated in *G. hirsutum* and *A. thaliana* by the VIGS method and overexpression of transformation, respectively. Our data indicated the conservation of m^{6}A methyltransferase (METTL) genes in cotton and provided inspirations for the divergent roles of *GhMETTL3* and *GhMETTL14* during the *Gossypium* evolution.

2. Results

2.1. Identification and Chromosomal Location of RNA Methyltransferase Genes in G. hirsutum

The N6-methyladenosine (m^6A) is the most abundant modification of mRNA in most eukaryotes [2]. Methyltransferases were the "writers" of m^6A, which included core METTL3 and METTL14 in humans [37]. Six methyltransferase-like genes (*METTL*) were identified in *G. hirsutum* genome by using Hmmersearch with conserved domains (PF05063 for mRNA: m^6A methyltransferase) (Table 1). These six *GhMETTL* genes were dispersed over 6 of the 26 *G. hirsutum* chromosomes with all homoeologs conserved (Fig. 1). Among them, *GH_A12G2586*/*GH_D12G2605* (*GhMETTL3_A*/*D*) were the homologs of *METTL3*, and *GH_A07G0817*/*GH_D07G0819* (*GhMETTL14_A*/*D*) were the homologs of *METTL14* in human. *GH_A06G0112*/*GH_D06G0096* were another two copies of methyltransferase-like genes in *G. hirsutum* (Figure 1).

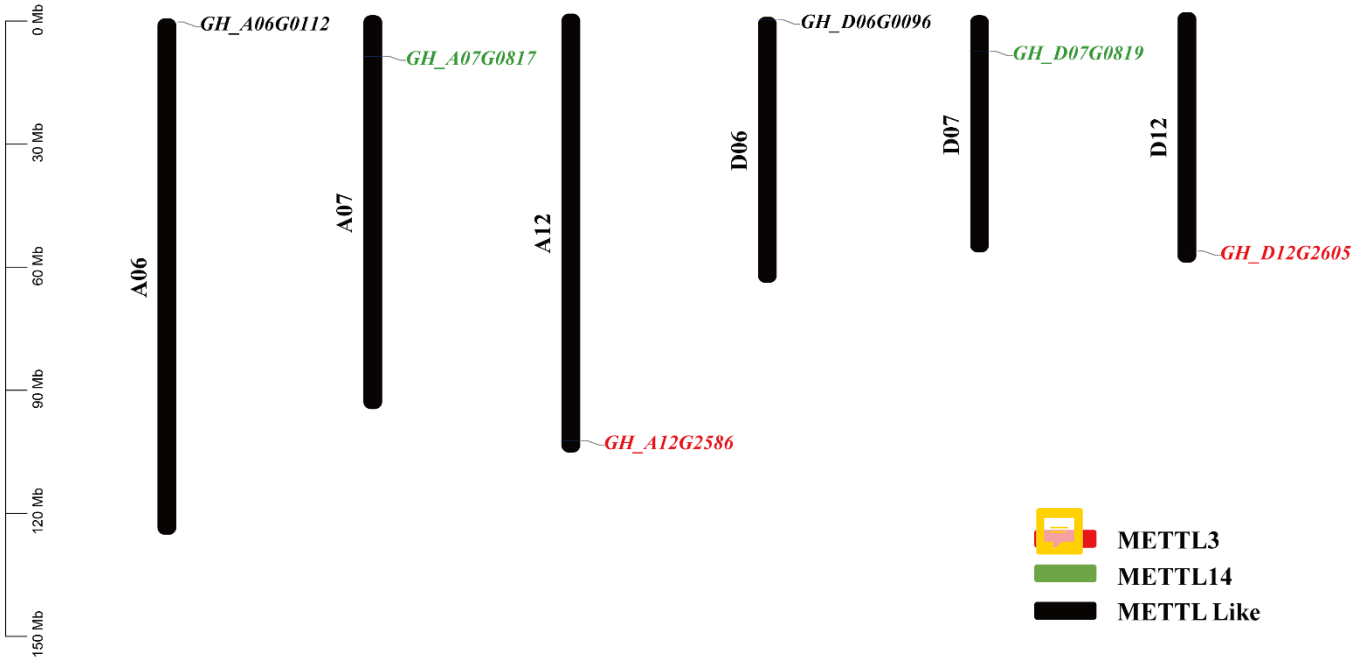

Figure 1. Dispersed distribution of METTL genes in *G. hirsutum* (AD1) chromosomes. 6 *GhMETTL* genes are scattered over 6 of the 26 *G. hirsutum* chromosomes.

2.2. Structural Organization of GhMETTL Genes

Less than threefold variation in length was detected in the predicted coding sequences (CDS) for these *GhMETTL*s, from 1,269 bp for *GH_A06G0112*/*GH_D06G0096* to 3,558 bp for *GH_A07G0817* (Table 1), which translates to proteins ranging from 422 amino acids (aa) (48.45 kDa) to 1185 aa (132.59 kDa). Predicted isoelectric points (pI) for members of this family range from 5.92 to 7.18 (Table 1). All putative *GhMETTL*s genes contain introns (Fig. S1), which exhibit considerable variations in length and number. In general, homoeologous *GhMETTL* genes show highly similar intron patterns; however, intron structure among homoeologous pairs can exhibit variation in intron number (5 to 8) and length (Fig. S1). One of the homoeologous gene pairs did exhibit divergence in intron length, namely the fourth intron of *GH_D12G2605* (*GhMETTL3_D*) was significantly less than that of *GH_A12G2586* (*GhMETTL3_A*). Characterizing the gene structure in the diploid parental species for the homoeologs suggests that the length variation of the fourth intron was not descendant divergence but inherited (Fig. S2). In addition, phylogenetic relationship of the *GhMETTL* gene family was consistent with the intron/exon structure characterized (Fig. S1).

Table 1. Sequence characteristics of *GhMETTL* (*G. hirsutum* methyltransferase) genes and protein

Gene Name	Locus Nam	Chr	Genomics Position	CDS	No. of Introns	Size (aa)	MW	pI
GhMETTL3_A	*GH_A12G2586*	A12	104,206,704-104,211,250	2,106	6	701	78.50	5.98
GhMETTL3_D	*GH_D12G2605*	D12	58,367,589-58,370,785	2,106	6	701	78.42	5.92
GhMETTL14_A	*GH_A07G0817*	A07	10,130,789-10,135,646	3,558	5	1185	132.59	7.10
GhMETTL14_D	*GH_D07G0819*	D07	8,927,821-8,932,500	3,555	5	1184	132.49	6.92
GhMETTLike_A	*GH_A06G0112*	A06	1,007,934-1,011,291	1,269	8	422	48.45	7.18
GhMETTLike_D	*GH_D06G0096*	D06	890,591-893,931	1,269	8	422	48.47	6.88

Note: bp: Base pair, Chr.: Chromosome, aa: Amino acid, MW: Molecular weight, kDa: Kilodalton, pI: Isoelectric point.

2.3. *Dynamic Evolution and Phylogenetic Analysis of METTL Genes in Gossypium*

We further evaluated the general preservation of METTL genes in 12 *Gossypium* species, *Gossypioides kirkii*, *Arabidopsis thaliana* and *Homo sapiens* (Figure 2). Two METTL genes (METTL3 and METTL14) were identified in *H. sapiens*. In *A. thaliana*, three METTL genes (AtMTA, AtMTB and AtMTC) were identified; the relative of *Gossypium*, *Gossypioides kirkii* has three METTL genes. 12 *Gossypium* species surveyed recovered a minimum of three putative METTL genes in diploid species and six in five allotetraploid species (Figure 2). Among D genome species, three METTL gene were identified in *G. thurberi* (D_1), *G. raimondii* (D_5) and *G. turneri* (D_{10}), respectively. The two cultivated diploid species of *G. herbaceum* (A_1) and *G. arboreum* (A_2) have four copies. The sister-species of A-genome *G. longicalyx* (F_1) contains three METTL genes. METTL copy numbers in the allotetraploid species surveyed were conversed with six METTL genes in five species: *G. hirsutum* (AD_1), *G. barbadense* (AD_2), *G. tomentosum* (AD_3), *G. mustelinum* (AD_4), *G. darwinii* (AD_5) (Figure 2). Notably, this high copy number in allotetraploid is almost double the copy number in diploid, likely reflective of the duplicated history of cotton. Comparatively, the METTL copy number is generally stable after polyploidization. The diploid A genome cotton species included here both appear to have undergone a homoeolog gain (3 versus 4).

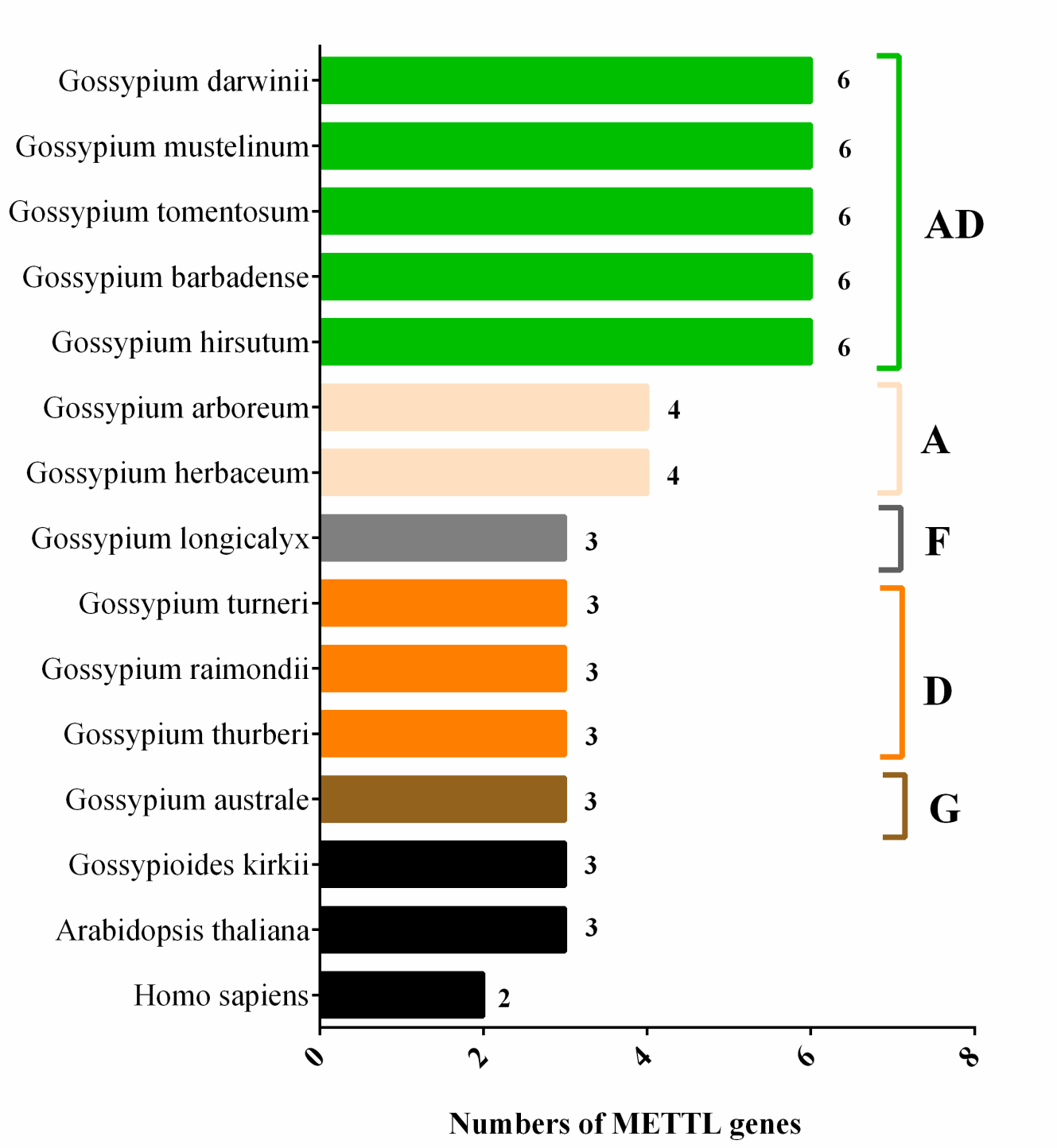

Figure 2. Dynamic evolution of the number of METTL family genes in 12 *Gossypium* species, *Gossypium kirkii*, *Arabidopsis thaliana*, and *Homo sapiens*.

To further investigate the evolutionary relationships between these METTL genes provided here, we specifically assessed this using the protein sequences of 61 METTL genes, including 53 *Gossypium*, 3 *Gossypioides kirkii*, 3 *A. thaliana* and 2 *H. sapiens* METTL genes for phylogenetic analysis (Figure 3). Three clades (METTL3, METTL14 and METTL Like) were robustly supported in *Gossypium* with one *A. thaliana* or *Gossypioides kirkii* gene associated with each clade, respectively, but shared METTL3 and METTL14 clades with *H. sapiens*.

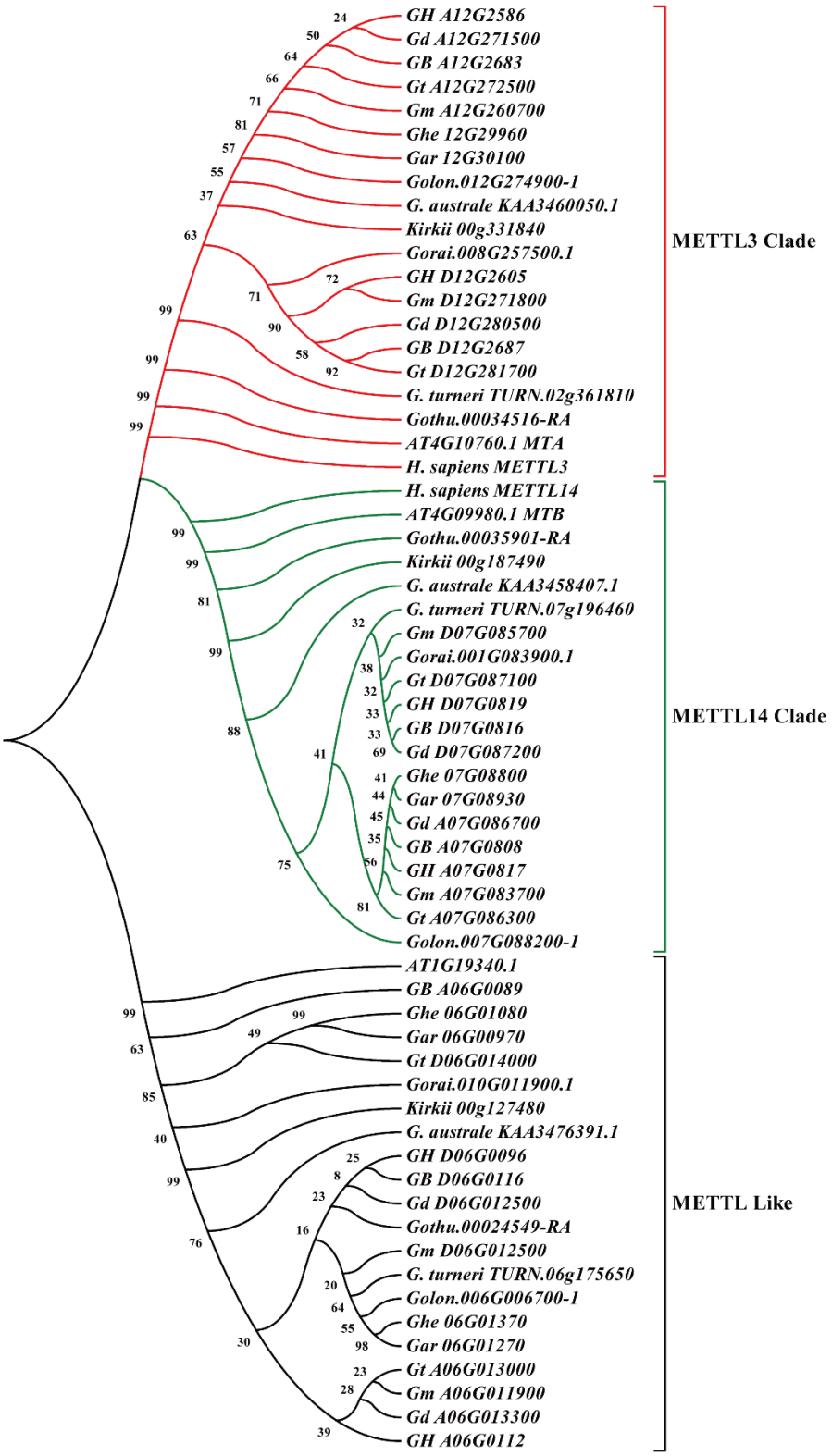

Figure 3. Phylogenetic analysis of METTL genes from 12 *Gossypium* species, *Gossypium kirkii*, *Arabidopsis thaliana*, and *Homo sapiens*. The phylogenetic tree was established with entire protein-coding sequences with NJ methods. The numbers on the branches indicate bootstrap support values from 1000 replications.

Overall, the expected diploid-polyploid topology is reflected in the tree for each set of orthologous/homoeologous genes, indicating general preservation during diploid

divergence and through polyploid evolution. That is, the number of METTL genes in allotetraploids was generally additive with respect to the model diploid progenitors, with each homoeolog (A_t or D_t) sister to their respective parental copies. METTL3 and METTL14 clades had the equal number of METTL genes (Figure 3). In clades METTL3 and METTL14, genes related to *AtMTA* and *AtMTB* were exhibited parallelly, and no duplication in *Gossypium* species, compared to the *A. thaliana* and *H. sapiens*. Therefore, it is speculated that the function of METTL genes in these clades of cotton is similar to that of the corresponding METTL genes in *Arabidopsis* and *H. sapiens*.

2.4. Cis-element Analysis of METTL Genes in G. hirsutum

Cis-elements are responsive to corresponding stimulations to regulate the expression of genes [38]. In this study, a 1.5-kb upstream region from the start codon of each METTL gene in *G. hirsutum* was extracted to investigate putative *cis*-elements involved in the mediation of gene expression using the PlantCARE server [39]. We totally identified 213 *cis*-elements among six *GhMETTL* genes, ranging from 24 in *GH_A12G2586* to 44 in *GH_D06G0096* (Fig. S3). All *GhMETTL* gene promoters had several TATA-box and CAAT-box elements (Fig. S3). Four *GhMETTL* gene promoters processed at least one abscisic acid responsiveness element (ABRE), and three *GhMETTL* genes had at least one AE-box (part of a module for light response in *A. thaliana*). *GhMETTL14_A* (*GH_A07G0817*) processed the element involved in HD-Zip 1 (involved in differentiation of the palisade mesophyll cells in *A. thaliana*). Six *GhMETTLs* had light responsiveness elements (GA-motif, GT1-motif and G box) and at least two MYB or one MYC binding site element (MYB/MYC). In addition, MYB-binding site involved in drought inducibility (MBS) also existed in these *GhMETTLs* genes.

2.5. Expression Patterns of GhMETTL Genes in Different G. hirsutum Tissues

The expression patterns of a gene family can provide valuable information to predict the possible biological functions of each gene. Analysis of six *GhMETTL* genes showed that most genes have different spatial expression patterns. For instance, the expression levels of *GhMETTL14* (*GH_A07G0817*/*GH_D07G0819*) and *GhMETTL3* (*GH_A12G2586*/*GH_D12G2605*) in root, stem, leaf, torus, petal, stamen, pistil and calycle were significantly higher than the other two *GhMETTL* like (*GH_A06G0112*/*GH_D06G0096*) genes (Figure 4A). *GhMETTL14* (*GH_A07G0817*/*GH_D07G0819*) and *GhMETTL3* (*GH_A12G2586*/*GH_D12G2605*) presented the highest expression level in pistil than other tissues (Figure 4A). In addition, *GhMETTL14* (*GH_A07G0817*/*GH_D07G0819*) still showed significant higher expression in seed and root samples at different time points after seed germination (Figure 4B). In ovule samples at different development stages, *GhMETTL14* (*GH_A07G0817*/*GH_D07G0819*) had the highest expression levels followed by *GhMETTL3* (*GH_A12G2586*/*GH_D12G2605*) (Figure 4C). In different development periods of fiber samples, *GhMETTL14* (*GH_A07G0817*/*GH_D07G0819*) had the highest expression in 20 and 25 dpa fiber cells (Figure 4D), suggesting that this gene might play an important role at the cell wall thickening stage. *GhMETTL3* (*GH_A12G2586*/*GH_D12G2605*) also presented higher expression in 20 and 25 dpa fiber cells than 5 and 10 dpa (Figure 4D). The above two genes were the homoeologs of the *H. sapiens METTL3* and *METTL14*, respectively (Figure 3). These results might suggest that *GhMETTL* genes may not be involved in the regulation of fiber cell elongation (Figure 4D). *GhMETTL3* and *GhMETTL14* might serve as the functional genes in charge of cotton fiber cell wall development.

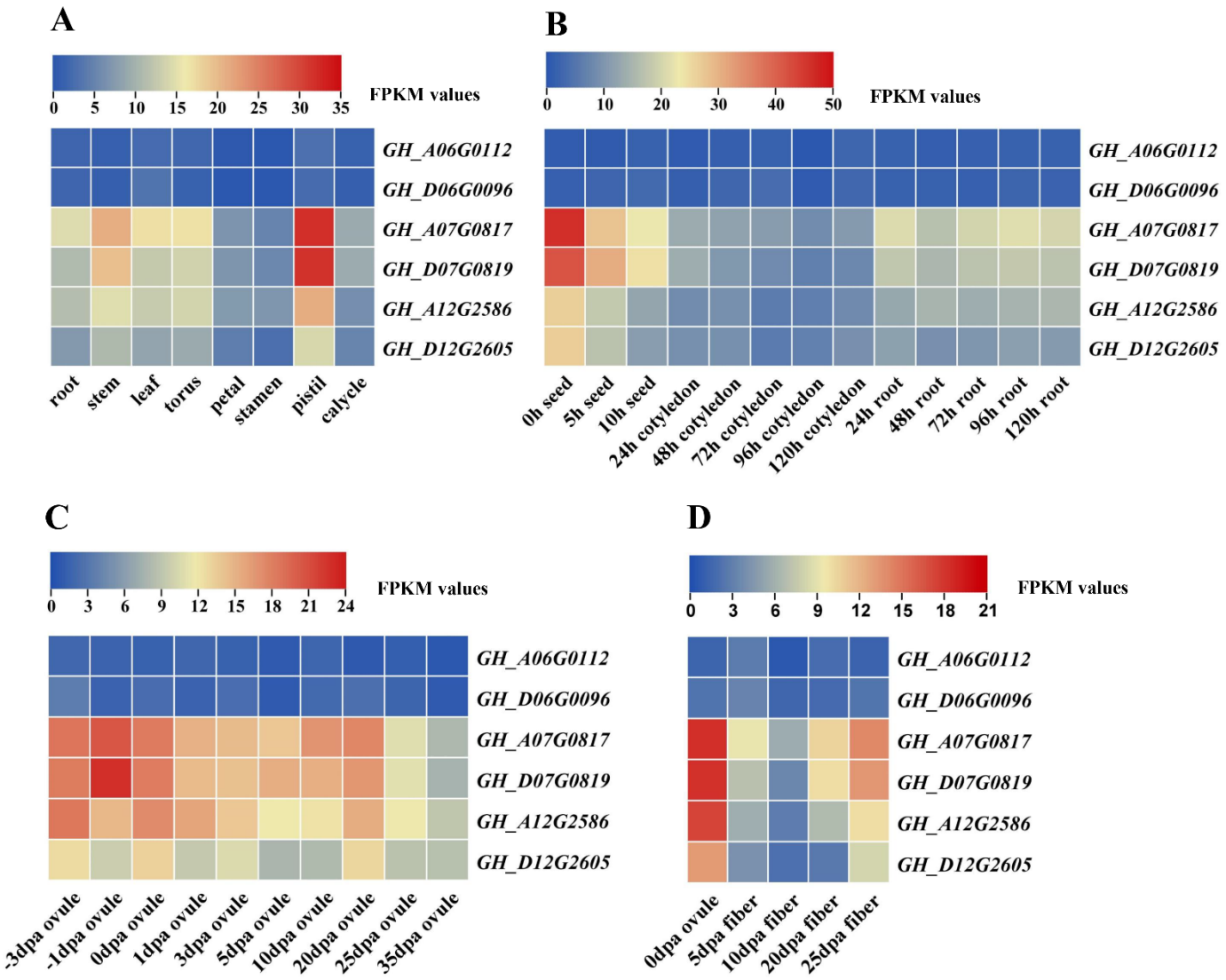

Figure 4. Expression patterns of *GhMETTL* genes in different cotton tissues and fiber cells of different stages based on the RPKM values of RNA-seq data. **(A)** Expression profiles of *GhMETTL* genes in eight cotton tissues. **(B)** Expression patterns of *GhMETTL* genes in seed germination, cotyledons and roots after germination. **(C)** Expression patterns of *GhMETTL* genes in ovules of different stages. **(D)** Expression patterns of *GhMETTL* genes in fibers of different stages.

2.6. Expression Changes of GhMETTL Genes in G. hirsutum under Different Stresses

A variety of abiotic stresses pose threatens to the growth and development of cotton plants. Therefore, we comprehensively analyzed the expression changes of *GhMETTL* genes under simulated drought (PEG 6000), salt (NaCl), heat and cold abiotic stresses from RNA-seq data (Figure 5). At different time points of PEG6000 simulation drought condition, the expression levels of six *GhMETTL* genes were slightly decreased but the difference was not significant ($|\lg_2$ (Fold change)$| \geq 1|$ as the threshold of differentially expressed genes). Among them, *GhMETTL14_A* (*GH_A07G0817*) gene was down-regulated after 1 h PEG treatment (Figure 5A) but not changed at the time points of 3, 6, and 12h. The expression of other *GhMETTL* genes did not change after PEG treatment for 1, 3, 6 and 12 h (Figure 5A). These results indicated that few *GhMETTL* genes were involved in response to drought stress in *G. hirsutum*. Meanwhile, at the four time points of salt or high temperature stress, the expressions of six *GhMETTL* genes both did not change after 1, 3, 6 and 12h of NaCl or hot treatment (Figure 5B, C).

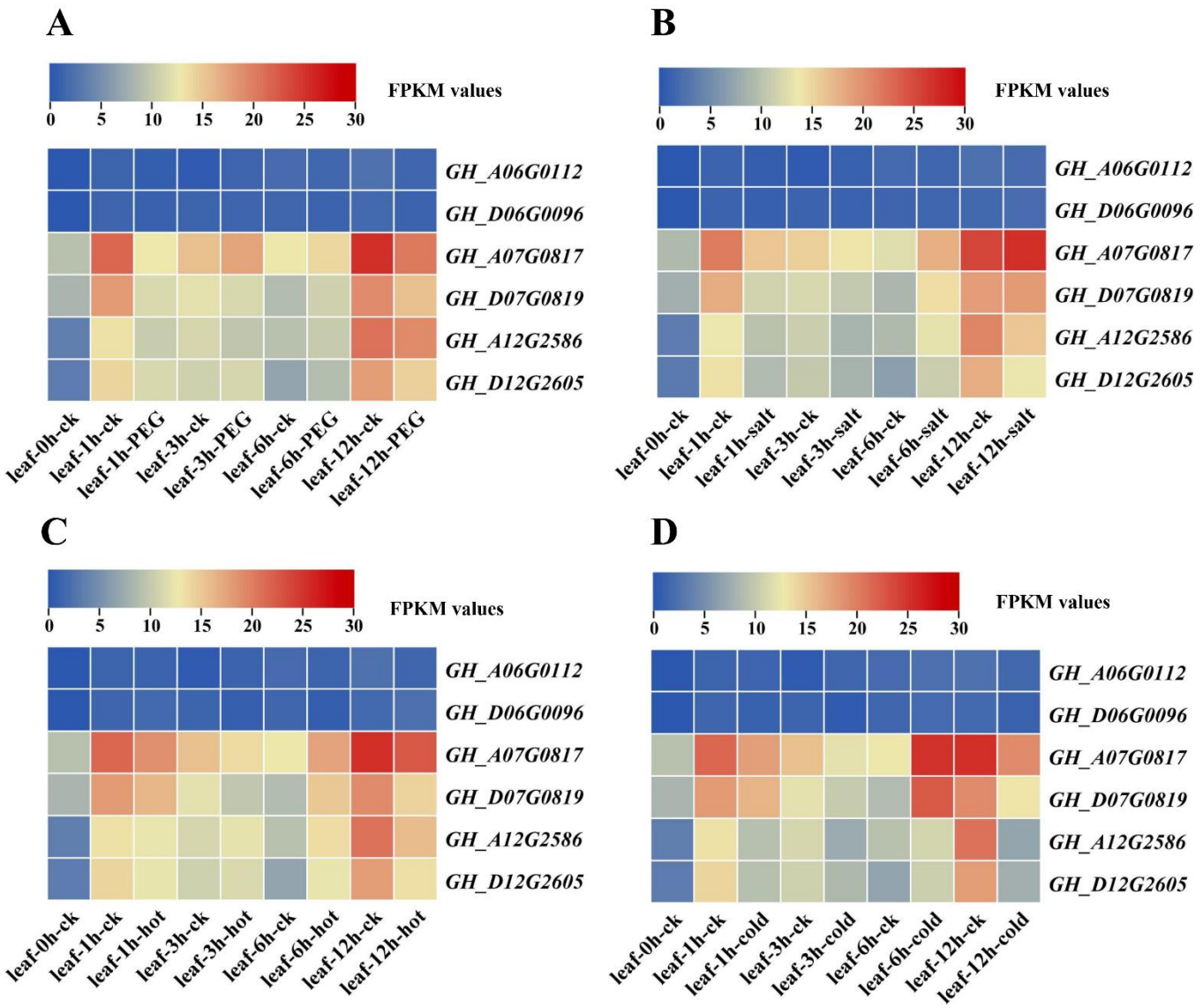

Figure 5. Expression patterns of *GhMETTL* genes in response to different stresses from RNA-seq data. The RNA-seq data were downloaded from Zhang et al., 2015 and re-analyzed the RPKM values of five time points (0, 1, 3, 6 and 12 h) after stresses treatments. **(A)** Drought stress; **(B)** Salt stress; **(C)** Hot stress; **(D)** Cold stress.

As for the four time points of low temperature stress in *G. hirsutum*, *GhMETTL14* (*GH_A07G0817*/*GH_D07G0819*) were up-regulated after 6 h of low temperature treatment (Figure 5D). However, the expressions of *GhMETTL3* (*GH_A12G2586*/*GH_D12G2605*) were repressed after 12 h low-temperature treatment. These results indicated their divergent regulating roles under low temperature stress. The expression levels of these genes did not change at other time points. The overall results showed that *GhMETTL3* and *GhMETTL14* played an important role in response to the adverse stress in cotton, which might be worth further exploring their biological functions.

2.7. Suppressing GhMETTL3 and GhMETTL14 Caused Development Arrest in G. hirsutum

To explore the role of the identified *GhMETTLs* during the development of cotton plants, virus-induced gene silencing (VIGS) approach was used to suppress the expression of *GhMETTL3* and *GhMETTL14* (Figure 6). About 400bp fragments from the conserved regions of both ~~two~~ genes were inserted into the tobacco rattle virus (TRV) vector, respectively, and TRV-vectors-carrying Agrobacterium strains were then co-inoculated into 1-week-old cotton plant cotyledons by the needleless syringe method. From those

silenced cotton plants, we selected each independent VIGS line for phenotypic analyses (Figure 6A-C). The qPCR results showed that the expression levels of *GhMETTL3* and *GhMETTL14* genes in silenced plants were significantly down-regulated (Figure 6D, E). Along with the decreased expression of the *GhMETTL* genes, suppressing *GhMETTL3* and *GhMETTL14* both caused development arrest in *G. hirsutum* with a more severe withered phenotype produced by *GhMETTL14* (Figure 6A). The resulting phenotypes also indicated that the inhibition of *GhMETTL14* resulted in slight yellowing leaves (Figure 6B). One month later, down-regulation of *GhMETTL3* and *GhMETTL14* by VIGS led to the death of cotton plants (Figure 6C). Then, the m^{6}A abundance from the leaf tissues of *GhMETTL3* and *GhMETTL14* VIGS plants were determined by quantitative mass spectrometry (MS) analysis (Figure 6F). For the TVR2 control leaf tissue, the m^{6}A/A ratio of total RNA was approximately 0.075% (Figure 6F), which was significantly higher than that in *GhMETTL3*-silenced and *GhMETTL14*-silenced plants ranging from 0.050% to 0.057% of m^{6}A/A ratio, respectively. Overall, the results showed that the decreased m^{6}A abundance might cause the growth arrest of *G. hirsutum* seedlings.

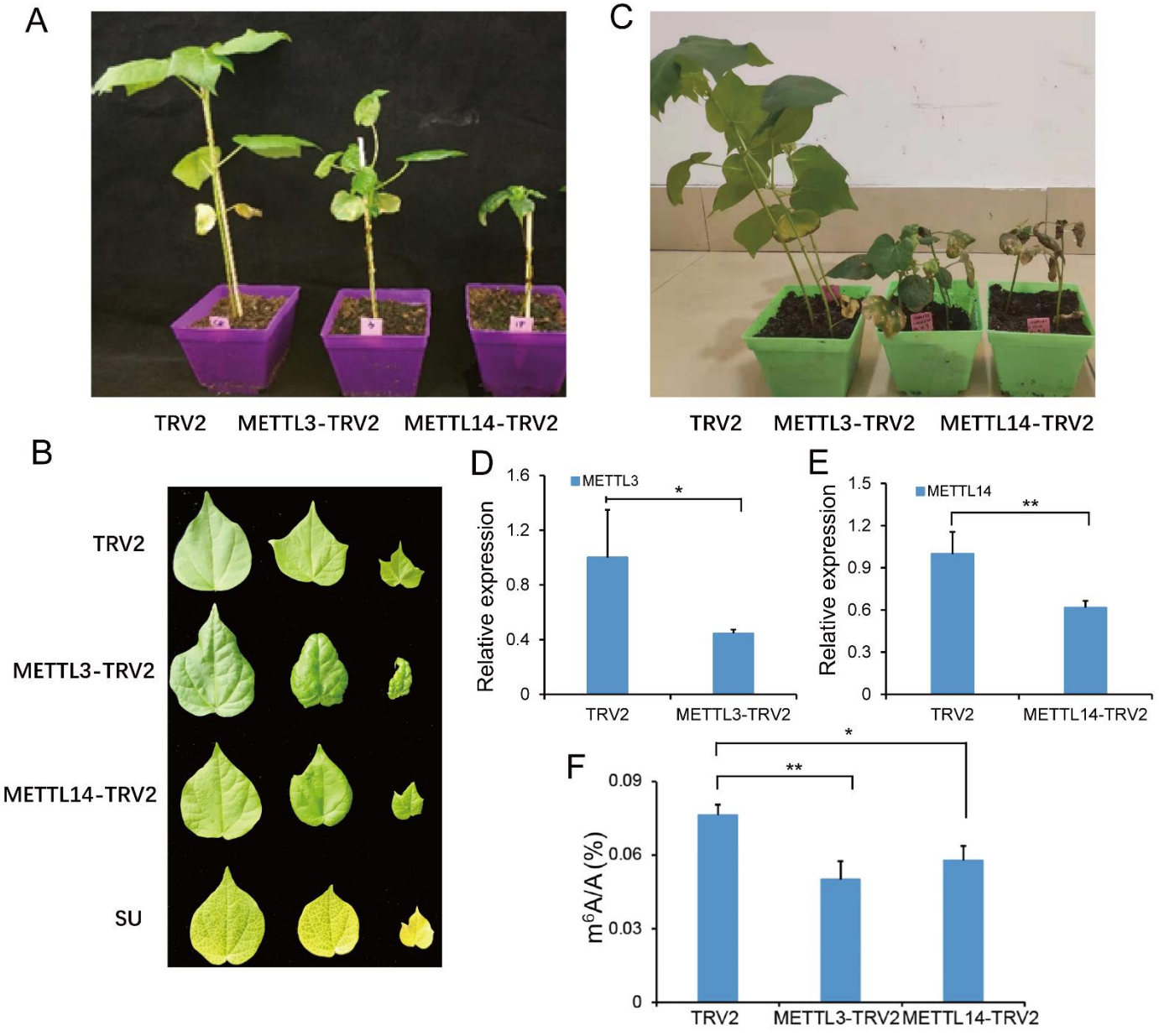

Figure 6. Suppressing *GhMETTL3* and *GhMETTL14* by virus-induced gene silencing (VIGS) approach. 400bp CDS fragments of two genes were inserted into the tobacco rattle virus (TRV) vector,

and TRV-vectors-carrying Agrobacterium strains were then co-inoculated into 1-week-old cotton plant cotyledons by the needleless syringe method. **(A)** Suppressing *GhMETTL3* and *GhMETTL14* both caused development arrest in *G. hirsutum*. **(B)** The leaf phenotypes of *GhMETTL3* and *GhMETTL14* VIGS cotton plants compared with the TRV2 blank vector plants. **(C)** Down-regulation of *GhMETTL3* and *GhMETTL14* by VIGS led to the death of cotton plants. **(D-E)** The qPCR data identified the repressed expression levels of *GhMETTL3* **(D)** and *GhMETTL14* **(E)** genes in silenced plants. **(F)** The decreased m^{6}A abundance from the leaf tissues of *GhMETTL3* and *GhMETTL14* VIGS plants determined by quantitative mass spectrometry (MS) analysis compared with the TVR2 control.

2.8. Subcellular Localization of GhMETTL3 and GhMETTL14 Proteins

To predict the subcellular localization of GhMETTL3 and GhMETTL14 proteins, we constructed two fusion vectors. A C-terminal fusion to GFP gene was generated, driven by the CaMV 35S promoter, to determine the subcellular localization. Then, GhMETTL3:GFP and GhMETTL14:GFP fusion proteins were transiently expressed in tobacco epidermal cells and viewed by a confocal fluorescence microscope (Figure 7). The transient expression of GhMETTL3:GFP and GhMETTL14:GFP fusion proteins were specifically localized in the nucleus, not other subcellular compartments. Combined with the m^{6}A ratio in the VIGS cotton, these results indicated that the GhMETTL3 and GhMETTL14 proteins act as the writers of m^{6}A in cotton.

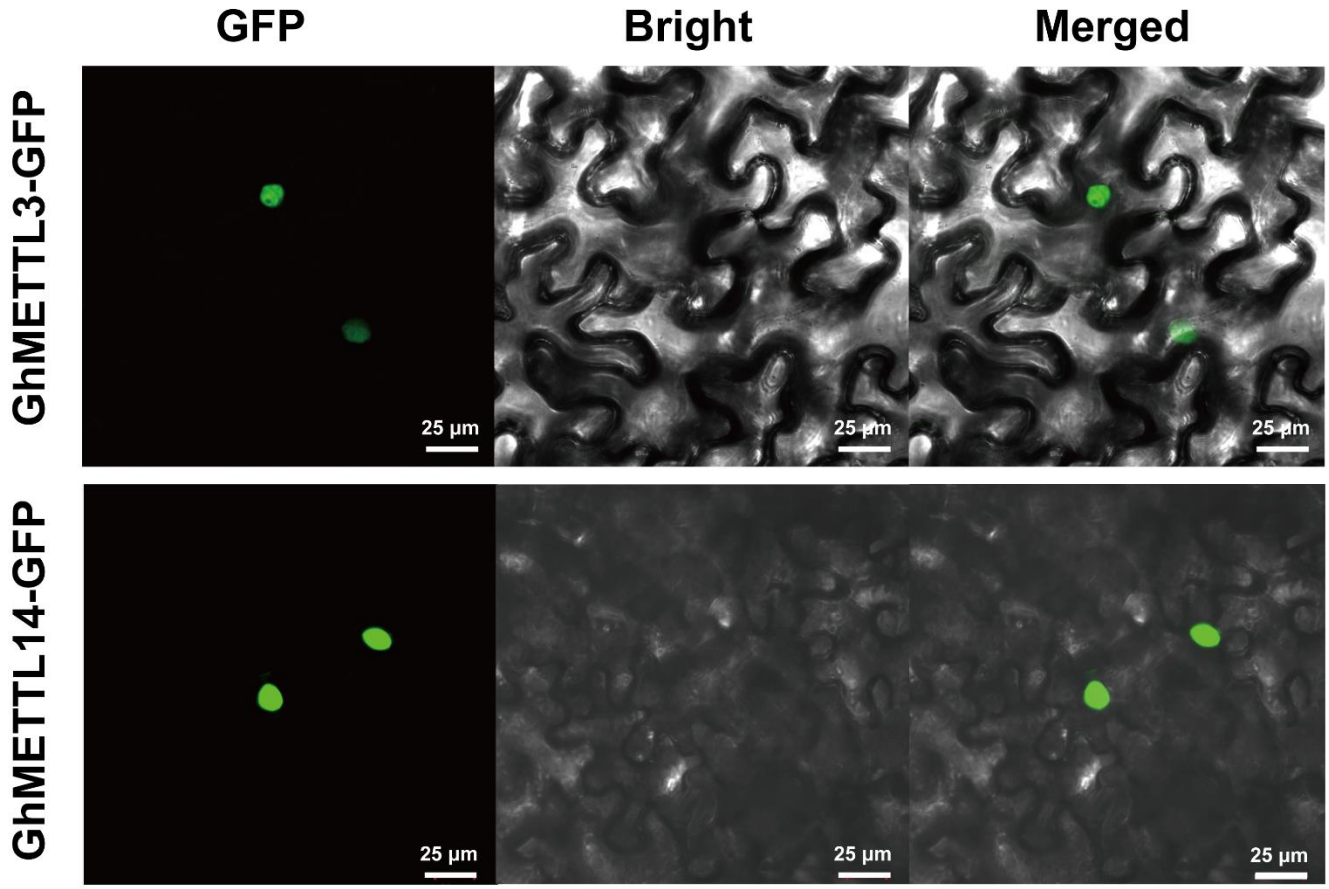

Figure 7. Subcellular localization assays of GhMETTL3 and GhMETTL14, showing nuclear localization of GhMETTL3-GFP (upper) and GhMETTL14-GFP (bottom). Agrobacterium cells harboring the fusion protein genes were infiltrated into leaves of *Nicotiana benthamiana* through the abaxial surface, and 72 h later the samples were observed under a confocal microscope (LSM510, Zeiss). Scale bar, 25 μm.

2.9. Overexpression of GhMETTL3 and GhMETTL14 Produced Distinct Differentially Expressed Genes (DEGs) in A. thaliana

To further analyze the biological function of *GhMETTL3 and GhMETTL14*, we transformed these two genes into *Arabidopsis* using the floral dip method, and then we obtained the T_1 generation transgenic plants. However, we did not observe any significant phenotypic difference between two transgenic and wild-type *Arabidopsis* plants during the whole growth period. To gain insights into the molecular mechanisms by overexpressing *GhMETTL3 and GhMETTL14* into *Arabidopsis* plants, we performed RNA-seq of leaf tissues from two transgenic plants compared with the wild-type.

Transcriptome data showed that there indeed existed differentially expressed transcripts in the leaf samples after transformation. In total, we identified 71 differentially expressed genes (DEGs) in *GhMETTL3* overexpressed *Arabidopsis* plants compared with the wild-type, among which 42 were induced and 29 were repressed (Figure S4A). Meanwhile, 1,274 DEGs were identified in *GhMETTL14* overexpressed *Arabidopsis* plants with 315 up-regulating and 958 down-regulating (Figure S4B).

Subsequently, these DEGs were subjected to KEGG pathway analysis to identify the functional categorization. Figure 8 lists the results of the KEGG analysis for DEGs. DEGs between *OEGhMETTL3* and WT were assigned to 17 KEGG pathways, including RNA degradation, phenylpropanoid biosynthesis, ascorbate and aldarate metabolism, inositol phosphate metabolism, protein processing in endoplasmic reticulum, nitrogen metabolism and MAPK signaling pathway – plant, etc. (Figure 8A). In addition, DEGs between *OEGhMETTL14* and WT were significantly enriched in 93 KEGG pathways, mainly including phenylpropanoid biosynthesis, glutathione metabolism, protein processing in endoplasmic reticulum, ascorbate and aldarate metabolism, starch and sucrose metabolism, pentose and glucuronate interconversions, pyruvate metabolism, fatty acid elongation, fatty acid biosynthesis, fatty acid degradation, nitrogen metabolism, RNA degradation, as well as MAPK signaling pathway - plant (Figure 8B). The above results revealed that these two methyltransferase genes (*GhMETTL3* and *GhMETTL14*) exerted extensive and distinct effects on the life processes in *A. thaliana* plant.

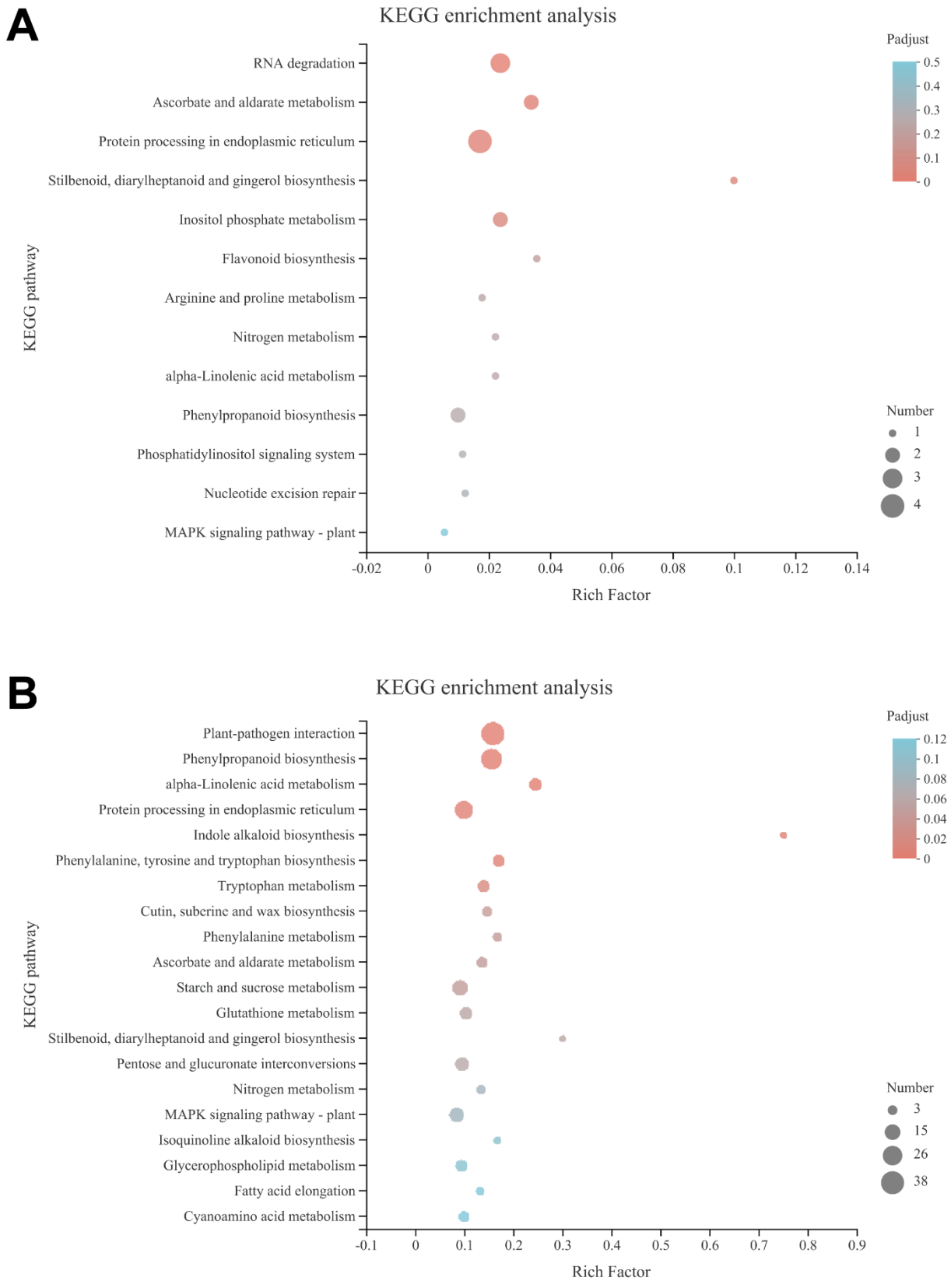

Fig. 8. KEGG pathway analysis of enriched differentially expressed genes in *OEGhMETTL3* and *OEGhMETTL14* plants compared with the wild type. **(A)** Top 13 pathways of significantly enriched DEGs between *OEGhMETTL3* and WT. **(B)** Top 20 pathways of significantly enriched DEGs between *OEGhMETTL14* and WT.

2.10. *GhMETTL3 and GhMETTL14 Exhibited Divergent Functions in Transgenic Arabidopsis*

Although no significant phenotypic changes were observed after these two genes were transformed into *A. thaliana*, transcriptome data still proved that *GhMETTL3* and *GhMETTL14* exhibited functional differentiation in transgenic *Arabidopsis*. We totally selected 88 genes that were differentially expressed between transgenic and wild-type *Arabidopsis*, and these DEGs could be classified into 11 families, including ethylene responsive transcription factor gene, bHLH transcription factor genes, WRKY transcription factor genes, dirigent protein genes, cytochrome P450 genes, calcium-binding protein genes, ABC transporter genes, glutathione S-transferase genes, detoxification genes, xyloglucan hydrolase genes, and CCR4-associated factor 1 homolog genes. Among them, six gene families: 9 ABC transporter genes (Figure 9A), 13 cytochrome P450 genes (CYP) (Figure 9B), 6 detoxification genes (DTX) (Figure 9C), 4 bHLH transcription factor genes (Figure 9D), 3 dirigent protein genes (DIR) (Figure 9E), and 9 glutathione S-transferase genes (Figure 9F) were all down-regulated in *OEGhMETTL14* transgenic *Arabidopsis* plants, but unchanged in *OEGhMETTL3* compared with the wild type plants. These results indicated that these two genes were functionally inconsistent.

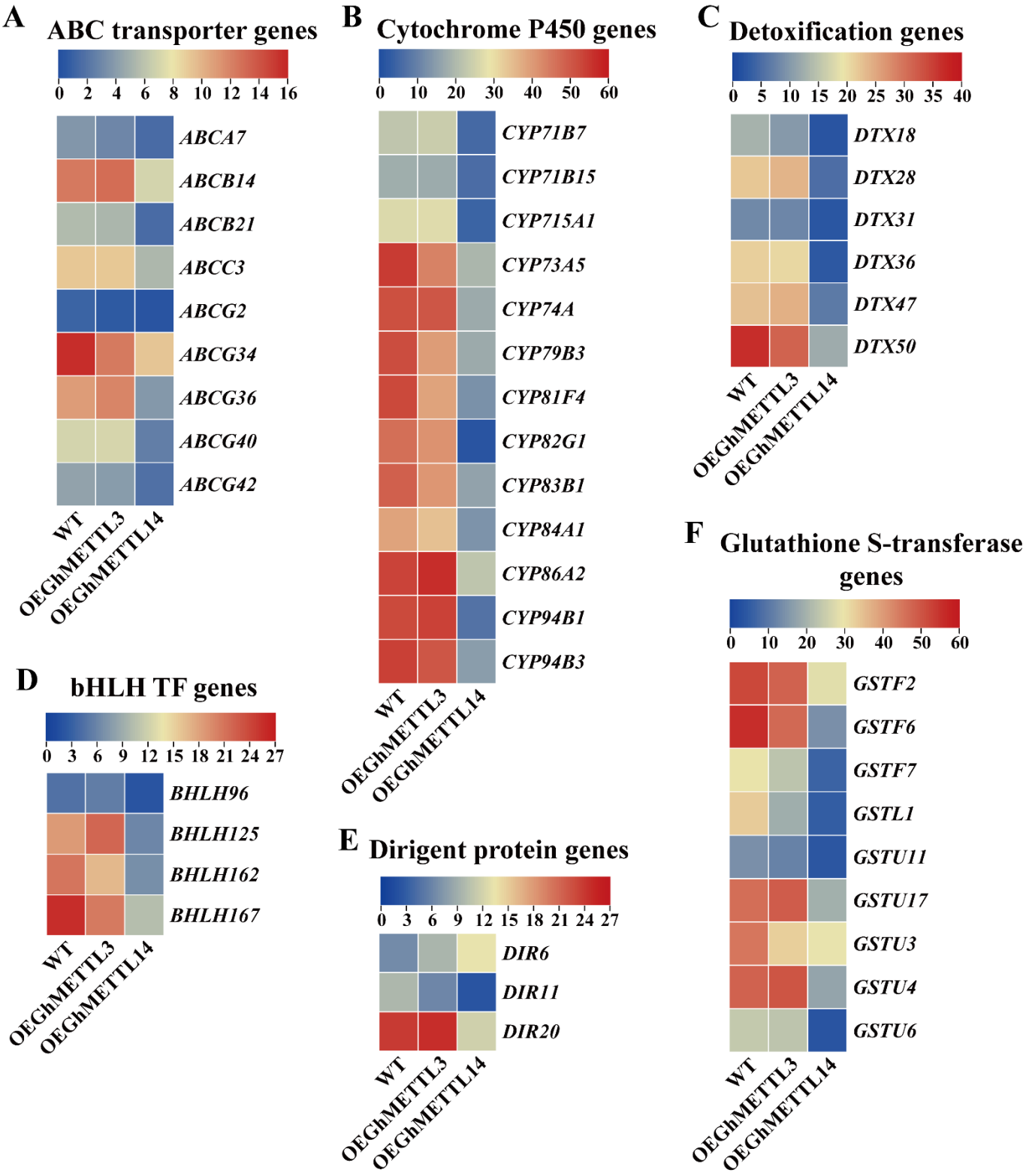

Figure 9. Expressions of six family genes were reduced in *OEGhMETTL14* but not changed in *OEGhMETTL3* transgenic *Arabidopsis* plants compared with the wild type. **(A)** ABC transporter genes, **(B)** cytochrome P450 genes (CYP), **(C)** detoxification genes (DTX), **(D)** bHLH transcription factor genes, **(E)** dirigent protein genes (DIR), **(F)** glutathione S-transferase genes.

In addition, among 13 calcium-binding protein (CML) genes (Figure 10A), the expression levels of eight *CML* genes (*CML12*, *CML27*, *CML39*, *CML41*, *CML42*, *CML44*,

CML46 and *CML47*) were down-regulated in *OEGhMETTL14* but not changed in *OEGhMETTL3* transgenic *Arabidopsis* plants compared with the wild-type. Four *CML* genes (*CML23*, *CML37*, *CML38*, and *CML40*) were repressed in *OEGhMETTL14* but induced in *OEGhMETTLL3* transgenic *Arabidopsis* plants. Expression of one *CML* gene (*CML45*) was increased in *OEGhMETTL3* but unchanged in *OEGhMETTL14* transgenic *Arabidopsis* plants (Figure 10A). For another 15-ethylene responsive transcription factor genes (ERF) (Figure 10B), there were six ERF genes (*ERF019*, *ERF043*, *ERF060*, *ERF061*, *ERF114*, and *ERF115*) being down-regulated in *OEGhMETTL14* plants compared with the wild-type, but not changed in *OEGhMETTL3*. Meanwhile, three ERF genes (*ERF1*, *ERF13* and *ERF1B*) were reduced in *OEGhMETTL14* but elevated in *OEGhMETTL3* plants. There still existed six ERF genes (*ERF5*, *ERF016*, *ERF017*, *ERF018*, *ERF104*, and *ERF105*) being up-regulated in *OEGhMETTL3* plants, but unchanged in *OEGhMETTL14* (Figure 10B). In addition, the presence of divergence between these two *GhMETTL* genes was also revealed from the expression patterns of 12 WRKY transcription factor genes (Figure 10C). Thereinto, the expressions of eight WRKY genes (*WRKY8*, *WRKY28*, *WRKY29*, *WRKY48*, *WRKY51*, *WRKY54*, *WRKY62* and *WRKY70*) were down-regulated in *OEGhMETTL14* compared with the wild-type, but not changed in *OEGhMETTL3*. Four WRKY genes (*WRKY33*, *WRKY40*, *WRKY46* and *WRKY53*) presented reduced expressions in *OEGhMETTL14*, but induced in *OEGhMETTL3* (Figure 10C). Expressions of three CCR4-associated factor 1 homolog genes (*CAF1-11*, *CAF1-5* and *CAF1-9*) were up-regulated in *OEGhMETTL3* plants, but not changed in *OEGhMETTL14* (Figure 10D). Finally, discordant expression patterns of four xyloglucan hydrolase genes (XTH) were also observed between *OEGhMETTL14* and *OEGhMETTL3* transgenic *Arabidopsis* plants (Figure 10E). Among them, the expressions of two *XTH* genes were up-regulated in *OEGhMETTL3* plants compared with that of wild type, but not changed in *OEGhMETTL14*. Two XTH genes exhibited repressed expressions in *OEGhMETTL14*, but up-regulated in *OEGhMETTL3* compared with the wild type (Figure 10E). The above results further confirmed that the incongruent expression levels of these differentially expressed genes caused by the transformations of *GhMETTL3* and *GhMETTL14* into *Arabidopsis thaliana*. Their biological functions might also be diverged and worth to be further explored in subsequent studies.

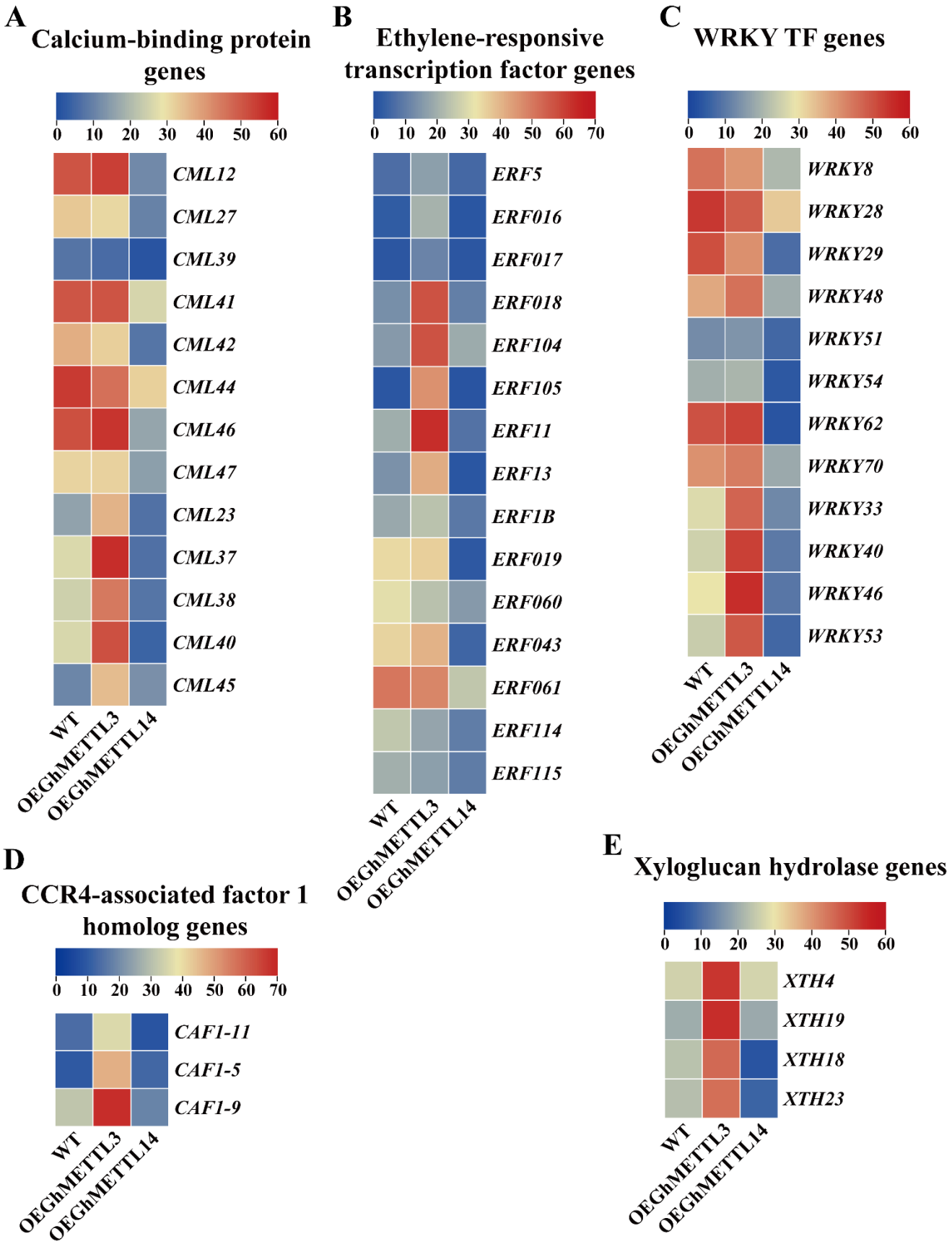

Fig. 10. Divergent expression patterns of five selected family genes between *OEGhMETTL3* and *OEGhMETTL14* transgenic *Arabidopsis* plants compared with the wild type. **(A)** calcium-binding protein (CML) genes, **(B)** ethylene responsive transcription factor (ERF) genes, **(C)** WRKY

transcription factor genes, **(D)** CCR4-associated factor 1 homolog genes (*CAF*), **(E)** xyloglucan hydrolase genes (XTH).

3. Discussion

N6-methyladenosine (m^6A) in RNA represents an indispensable post-transcriptional modification in gene regulation. It was involved in RNA stability and degradation [40], mRNA alternative splicing [41], affected the translation efficiency [42] and miRNA processing [43]. Meanwhile, the m^6A modification plays a critical role in plant growth, development and response to the adverse environmental stresses. The m^6A writer components included MTA, MTB, FIP37, VIRILIZER and HAKAI in *A. thaliana* [3, 44-46]. When the expression level of m^6A writer components, such as m^6A methyltransferase was reduced, the abundance of m^6A also showed a dramatic reduction [11]. Knockout of m^6A methyltransferase MTA prevent development and eventually led to embryonic lethality while inactivation of other writer components the increasing trichome branches phenotypes, as well as the over-proliferation of shoot apical meristem [3, 44, 45].

Previous reports have indicated that m^6A modification were involved in abiotic and biotic stress responses [47-50]. The increase of 5′ UTR m^6A level would promote the protein translation in response to the heat shock stress [51]. Another study showed that m^6A methylation was involved in salt stress tolerance in *Arabidopsis*. Both mutants of m^6A writer components, such as MTA and MTB, displayed salt-sensitive phenotypes along with the reduced m^6A level [52]. On the other hand, the m^6A methylation level showed a reduction after exposure to virus infection in *Nicotiana tabacum* and drought stress in *Zea mays*, respectively [53, 54]. In addition, the expression of m^6A methyltransferase *ClMTB* in watermelon was also induced by drought stress. Overexpression *ClMTB* into tobacco plants increased its drought tolerance by enhancing ROS scavenging activity [14]. Overexpressing a *Populus trichocarpa* m^6A methyltransferase also enhanced the tolerance to drought stress by increasing the trichome and root density in poplar [12]. In our study, we also found the expression of *GhMETTL14_A* (*GH_A07G0817*) gene was repressed after simulated drought PEG treatment. These results indicated that METTL genes mediated m^6A modification were involved in response to environmental stresses in plants.

For the emergence of homologous genes in a single gene family after duplication, homologous genes generally have different fates: both genes retained for dosage effect, or diverged to produce new function [55, 56]. In METTL3 mutants, the translation of mRNAs containing m^6A modifications in the 5′UTR was reduced, indicating translation efficiency was influenced by 5′UTR m^6A in cells [57, 58]. Early reports also found that m^6A modifications in 5′UTR regions were positively correlated with gene expression in Arabidopsis [59]. These investigations suggested that the METTL3 protein was the most-active m^6A methyltransferase enzyme to catalyze m^6A RNA methylation and a core m^6A methyltransferase component. However, studies found that METTL14 have no methyltransferase activity, but could form a stable antiparallel heterodimer with METTL3 to further bind to the RNA substrates in cells [7-9]. In Arabidopsis, AtMTA protein was necessary for the m^6A mRNA methylation, and loss of function led to plant embryo development arrest, further to lethality [11]. However, the function of AtMTB identified might have no m^6A methyltransferase activity in Arabidopsis [13]. Further, only one METTL3 or MTA homologous protein was identified in barley and *Micromonas pusilla*. In these two species, the METTL14 or MTB protein may have undergone a functional gene loss during evolution or evolved to a distinct molecular role of new gene family but not the MT-A70-like protein [3]. In our study, the similar phenomenon of GhMETTL gene's function divergence was observed in *Gossypium*. For instance, the expressions of *GhMETTL14* (*GH_A07G0817*/*GH_D07G0819*) were induced after low temperature treatment, but *GhMETTL3* (*GH_A12G2586*/*GH_D12G2605*) were repressed under low-temperature stress. Meanwhile, *GhMETTL3* and *GhMETTL14* also exhibited divergent functions in transgenic *Arabidopsis* based on the transcriptome data. Compared to the wild-type type,

the expressions of DEGs between *OEGhMETTL3* and *OEGhMETTL14* transgenic *Arabidopsis* were always inconsistent. These results implied that the homologous genes in a single gene family, such as m^{6}A methyltransferases METTL3 and METTL14, had divergent regulatory roles during the process of growth and development of plants and animals.

Although there have been many studies on the response of METTL in regulating plant growth and development as well as responses to adverse stresses in plants, there are few studies on the exploration the potential roles of *METTLs* in cotton. The overall results of this study showed that *GhMETTL3* and *GhMETTL14* played different roles in cotton, which is worth further exploring their biological functions with modern biotechnologies such as gene editing.

4. Materials and Methods

4.1. Identification of METTL Family Genes and METTL Proteins in Diploid and Tetraploid Gossypium Species

The genome sequences of cotton species were downloaded from the CottonGen database [60], including *G. raimondii* [19], *G. herbaceum* [25], *G. arboreum* [23], *G. hirsutum* [28], *G. barbadense*, *G. tomentosum*, *G. mustelinum* and *G. darwinii* [25, 28-35]. To identify all putative METTL proteins in each genome assembly, the METTL protein conserved domains (PF05063 for MTA70 superfamily) were used to develop a Hidden Markov Model [61] profile matrix via the hmmbuild program from the HMMER package [62] with default parameters. This HMM profile matrix was used in conjunction with hmmersearch with default parameters against these *Gossypium* genome databases to identify putative METTL genes (*GhMETTLs*) [63, 64]. Previously identified METTL gene sequences from *A. thaliana* (*AtMTA* and *AtMTB*) and *H. sapiens* (METTL) were retrieved from the TAIR database [65] and NCBI database (https://www.ncbi.nlm.nih.gov) for phylogenetic comparison, respectively. The presence of conserved domains in each *Arabidopsis* and Gossypium gene was verified by the SMART conserved domain search tool [66] and Pfam databases [67].

4.2. Chromosomal Location and Gene Structure Analyses

Chromosomal locations for the identified *GhMETTLs* were extracted from the genome annotation gff3 file [28, 34]. Chromosomal locations of the predicted *GhMETTLs* was visualized using TBtools [68], and the exon-intron structure of each gene was displayed using the online tool GSDS 2.0 [69]. The number of amino acids, molecular weight (MW), and theoretical isoelectric point (pI) of putative *GhMETTLs* proteins were determined using the ProtParam tool [70].

4.3. Sequence Alignment and Phylogenetic Tree Construction

Complete protein-coding sequences for *METTL* genes from 12 *Gossypium* species, *Gossypioides kirkii*, *A. thaliana* and *H. sapiens* were aligned using MAFFT with the G-INS-i algorithm [71]. The NJ phylogenetic tree was constructed using MEGA version 6.0 [72] by sampling 1000 bootstrap replicates.

4.4. Analysis of Cis-acting Element in Promoter Regions of GhMETTLs

The upstream sequences (1.5 kb) [73] of the *GhMETTLs* genes were retrieved from *G. hirsutum* genome sequence based on the gene locations [28, 34]. Then, the retrieved promoter sequences were submitted to PlantCARE [39] to identify the potential *Cis*-acting element.

4.5. Expression Patterns of GhMETTLs in Different Tissues and Stress Conditions

Raw RNA-Seq data for *G. hirsutum* seed, root, stem, leaf, torus, petal, stamen, ovary, calyx, ovule (-3 dpa, -1 dpa, 0 dpa, 1 dpa, 3 dpa, 5 dpa, 10 dpa, 20 dpa, 25dpa, 35dpa) and fiber (5 dpa, 10 dpa, 20 dpa, 25dpa) were downloaded from the NCBI Sequence Read Archive (PRJNA 248163) [28, 34], represented by one library each. Reads were mapped to *G. hirsutum* genome [34] via HISAT2 software with default parameters, and read abundance with calculated via StringTie [74, 75]. Read counts were normalized in R3.2 using RUVSeq [76] and the internal control reference gene *GhUBQ7*, which is detected at relatively constant levels across different cotton samples [77]. Potential batch-effects were corrected by

an improved version of ComBat, ComBat-seq [78]. Gene expression was estimated by Ballgown [86], using fragments per kilobase million (FPKM) values to calculate the gene expression levels across libraries. Expression levels of *G. hirsutum* leaf RNA-Seq data (in FPKM) for each *GhMETTL* gene under drought, salt, heat and cold stress (time points: 0, 1, 3, 6, 12h) were retrieved from the ccNET database [79]. Genes were considered differentially expressed if expression varied more than two-fold change with a p-value of less than 0.05. TBtools [68] was used to display the gene expression patterns from the calculated FPKM values [80].

4.6. Virus-Induced Gene Silencing (VIGS) Assays

The virus-induced gene silencing (VIGS) assays were finished based on previous reports [81-83]. Briefly, to knockdown the expression of the GhMETTL genes, about 400-bp fragment of the *GhMETTL3* and *GhMETTL14* cDNA from upland cotton R15 was PCR-amplified using specific primers (Table S1). The resulting PCR products were infused to pTRV2 to produce the VIGS vectors named pTRV2-*GhMETTL3* and pTRV2-*GhMETTL14*, respectively. The pTRV1 and pTRV2-*GhMETTL3* or pTRV2-*GhMETTL14* vectors were introduced into the Agrobacterium strain GV3101 through electroporation (Bio-Rad, Hercules, CA, USA). For the VIGS assay, the transformed Agrobacterium colonies containing pTRV1 and pTRV2-*GhMETTL3* or pTRV2-*GhMETTL14* were grown overnight at 28 °C. The Agrobacterium cells were collected and resuspended in the infiltration medium (10 mM MgCl2, 10 mM MES and 200 mM acetosyringone) and subsequently adjusted to an OD600 of 0.5. The Agrobacterium strains containing the pTRV1 and pTRV2-*GhMETTL3* or pTRV2-*GhMETTL14* vectors were mixed at a ratio of 1:1. Cotton seedlings with mature cotyledons but without a visible rosette leaf (7 days after germination) were infiltrated by inserting the Agrobacterium suspension into the cotyledons via a syringe. The plants were then grown at 22 °C in pots arranged in a growth chamber under a 16-h light-8-h dark cycle and at a humidity rate of 60%. The mutant of *GhSU* has an obvious leaf yellowing phenotype during seeding stage and we used *GhSU* as the positive control for VIGS.

4.7. RNA Extraction, cDNA Synthesis and qRT-PCR Expression Analyses

These experiments were conducted with the methods reported before [84-86]. In brief, total RNAs from cotton leaf were extracted using a RNAprep pure plant kit (TIANGEN, Shanghai, China). The resulting RNAs were treated with DNase I prior to synthesizing cDNA with oligo (dT) primers and M-MLV Reverse Transcriptase (Invitrogen); these products were diluted 5-fold before use. For quantitative real-time PCR (qRT-PCR), Primer5 software was used to design gene-specific forward and reverse primers (Table S1). Analyses were performed with SYBR-Green PCR Mastermix (TaKaRa) on a cycler (Mastercycler RealPlex; Eppendorf Ltd, Shanghai, China). The *G. hirsutum histone-3* (*GhHIS3*) genes were used as internal references, and the relative amount of amplified product was calculated following the $2^{-\Delta\Delta Ct}$ method [87].

4.8. Quantitative Analysis of m⁶A Level in Cotton Leaf Tissue

The quantification of m⁶A level in cotton leaf was referred to the methods of a previous report [88]. In detail, mRNA was extracted from 10 μg total RNA for each sample with Dynabeads™ mRNA Purification Kit (Invitrogen, 61006). Then, 150 ng purified RNA was digested by 1 U nuclease P1 (Sigma, N8630) in containing 10 mM NH_4Ac reaction buffer up to 20 μL at 42°C for 3 h. Subsequently, 1 U rSAP (NEB, M0371S) and 5 μL rCutSmart buffer were added to the mixture,incubated at 37°C for additional 6 h. 1 μL digested RNA was injected into a LC-MS/MS (AB SCIEX QTRAP 5500) to detect the mononucleotide. The m⁶A level was detected and quantified in the positive ion multiple reaction-monitoring (MRM) mode with the nucleoside to base ion mass transitions (282.0 to 150.1 for m⁶A and 268.0 to 136.0 for A). The concentrations of m⁶A level in cotton leaf were calculated from the standard curve generated from pure nucleoside standards.

4.9. Subcellular Localization of GhMETTL3 and *GhMETTL14 Proteins and Microscopic Observation*

The protein subcellular localization experiments were carried out as described in the previous study [89]. The coding region of GhMETTL3 and GhMETTL14 was fused to GFP

by PCR. The vectors carrying p35S::GhMETTL3-GFP and p35S::GhMETTL14-GFP were introduced into Agrobacterium cells, which were infiltrated with a syringe into the abaxial surface of *N. benthamiana* leaves for transient expression. Three days later, the infiltrated areas were observed under a confocal microscope (LSM510, Zeiss).

4.10. Arabidopsis Transformation

The floral-dip method was used for Arabidopsis transformation [90]. In brief, to overexpress the gene *GhMETTL3* and *GhMETTL14* in *A. thaliana*, the full-length cDNA of *GH_A12G2586* (*GhMETTL3_A*) and *GH_A07G0817* (*GhMETTL14_A*) was cloned into the pCAMBIA2301 vector driven by the CaMV35S promoter, respectively. This recombinant plasmid was transferred into Agrobacterium cells and then transformed into *A. thaliana* plants via the floral dip method [90, 91]. Kanamycin painting and PCR analysis confirmed the transgenic lines.

4.11. RNA Sequencing of OEGhMETTL3, OEGhMETTL14 and Wild Type A. thaliana Plants

Total RNA was isolated from the OEGhMETTL3, OEGhMETTL14 and wild type *A. thaliana* plants. Library construction and sequencing were performed following the previous reports [92, 93]. In detail, 1 μg of purified mRNA was selected for cDNA library construction. mRNA was purified from total RNA using poly-T oligo-attached magnetic beads. cDNA fragments 240 bp in length were preferentially selected, and the library fragments were purified with an AMPure XP system (Beckman Coulter, Beverly, USA). Finally, the PCR products were purified (AMPure XP system), and library quality was assessed on an Agilent Bioanalyzer 2100 system. After cluster generation, the library preparations were sequenced on an Illumina HiSeqTM 2500 platform, and 150 bp paired-end reads were generated. Three biological replicates were performed for the transgenic and wild type *A. thaliana* plants.

4.12. Read Data Quality Control, Mapping and Calculations of the Differentially Expressed Genes

Raw data (raw reads) in fastq format were first processed through FASTX-Toolkit (http://hannonlab.cshl.edu/fastx_toolkit/). Clean data (clean reads) were obtained by removing reads containing adapters, reads containing poly-N sequences and low-quality reads from the raw data. The downstream analyses were based on clean high-quality data. RNA-seq data were mapped to the reference genomes using HISAT2 software [74, 75]. Only reads with a perfect match or one mismatch were further analyzed to calculate the expression values. Differential expression analysis of the two groups was performed using DESeq2 [94]. The resulting p values were adjusted using Benjamini and Hochberg's approach for controlling the false discovery rate (FDR). Genes with an adjusted p value < 0.01 and twofold change (up and down) were defined as differentially expressed. TBtools [68] was used to display the gene expression patterns from the FPKM values.

4.13. Gene Annotation and Enrichment Analyses

Differentially expressed gene functions were annotated based on the following databases: Nr (NCBI nonredundant protein sequences, ftp://ftp.ncbi.nih.gov/blast/db/), Nt (NCBI nonredundant nucleotide sequences, ftp://ftp.ncbi.nih.gov/blast/db/), and Kyoto Encyclopedia of Genes and Genomes (KEGG) (http://www.genome.jp/kegg/). KOBAS was used to test the statistical enrichment of the differentially expressed genes in the KEGG pathways [95].

5. Conclusions

We reported the structures, domains, phylogenetics, divergence, and *cis*-elements analyses systematically of *Gossypium METTL* genes. We also investigated the expression patterns of METTL family genes in different cotton tissues and under different stress conditions to predict their possible biological functions. Both *GhMETTL3* and *GhMETTL14* genes were variably expressed in different cotton tissues with particularly high expression in pistil and ovules. Suppressing *GhMETTL3* and *GhMETTL14* by VIGS would lead to the development arrest in *G. hirsutum*. Overexpression of *GhMETTL3* and *GhMETTL14* into Arabidopsis did not produce significant phenotypes difference but effected the expressions of variant family genes, implying their divergent functions in the regulation of

growth and development of cotton plants. Together, our results provide candidate genes to facilitate the functional identification of the METTL genes in subsequent study.

List of Abbreviations: METTL: m^{6}A methyltransferase; DEGs: Differentially expressed genes; FPKM: Fragments per kilobase of transcript per million mapped fragments; *G. herbaceum*: *Gossypium herbaceum*; *G. arboreum*: *Gossypium arboreum*; *G. longicalyx*: *Gossypium longicalyx*; *G. thurberi*: *Gossypium thurberi*; *G. raimondii*: *Gossypium raimondii*; *G. turneri*: *Gossypium turneri*; *G. australe*: *Gossypium austral*; *G. hirsutum*: *Gossypium hirsutum*; *G. barbadense*: *Gossypium barbadense*; *G. tomentosum*: *Gossypium tomentosum*; *G. mustelinum*: *Gossypium mustelinum*; *G. darwinii*: *Gossypium darwinii*; *A. thaliana*: *Arabidopsis thaliana*; *Homo sapiens*: *H. sapiens*; MW: Molecular weight; pI: Isoelectric point; qRT-PCR: Quantitative real-time polymerase chain reaction

Supplementary Materials: The following supporting information can be downloaded at: www.mdpi.com/xxx/s1, Figure S1: title; Table S1: title.

Figure S1. Phylogenetic tree and gene structure of METTL protein genes in *G. hirsutum*. Exons and introns are represented by yellow boxes and black lines, respectively.

Figure S2. Gene structure of *GhMETTL3* homoeologs in the diploid parental species. Exons and introns are represented by yellow boxes and black lines, respectively.

Figure S3. *Cis*-elements in promoter regions of *GhMETTL* genes.

Figure S4. Volcano plot exhibited the differentially expressed genes (DEGs) in *GhMETTL3* **(A)** and *GhMETTL14* **(B)** overexpressed *Arabidopsis* plants compared with the wild-type. The red and green dots represent the upregulated or downregulated genes, respectively.

Table S1. List of forward and reverse primers used for this study.

Author Contributions: Conceptualization, X.SG. and Z.C.; methodology, J.C.; software, C.H.; validation, J.C., C.H. and Z.Z.; formal analysis, L.H. and C.L.; investigation, X.L. and J.H.; resources, J.L.; data curation, J.C.; writing—original draft preparation, J.C. and Z.C.; writing—review and editing, Z.C.; visualization, L.W. and Y.Z.; supervision, Z.C.; project administration, Z.C.; funding acquisition, Z.C. All authors have read and agreed to the published version of the manuscript.

Funding: This work reported in this publication was supported by the Hainan Yazhou Bay Seed Laboratory (B22E49716, B22C39101), the Basic Research Program of Shanxi Province (20210302123409). The funding bodies did not participate in the design of the study and collection, analysis, and interpretation of data and in writing the manuscript.

Institutional Review Board Statement: Not applicable.

Informed Consent Statement: Not applicable.

Data Availability Statement: RNA-sequencing data that support the findings of this study have been deposited in the Genome Sequence Archive in the BIG Data Center of Sciences (https://bigd.big.ac.cn/) under accession CRA005794.

Acknowledgments: We thank Prof. Tian-Zhen Zhang for providing the RNA-seq expression data of the RPKM values and Prof. Xiao-Ya Chen for discussions.

Conflicts of Interest: The authors declare no conflicts of interest.

References

1. Liu, N.; Pan, T., N6-methyladenosine-encoded epitranscriptomics. *Nat Struct Mol Biol* **2016,** 23, (2), 98-102.
2. Zhou, L.; Gao, G.; Tang, R.; Wang, W.; Wang, Y.; Tian, S.; Qin, G., m(6) A-mediated regulation of crop development and stress responses. *Plant Biotechnol J* **2022,** 20, (8), 1447-1455.

3. Yue, H.; Nie, X.; Yan, Z.; Weining, S., N6-methyladenosine regulatory machinery in plants: composition, function and evolution. *Plant Biotechnol J* **2019,** 17, (7), 1194-1208.
4. Bokar, J. A.; Shambaugh, M. E.; Polayes, D.; Matera, A. G.; Rottman, F. M., Purification and cDNA cloning of the AdoMet-binding subunit of the human mRNA (N6-adenosine)-methyltransferase. *RNA* **1997,** 3, (11), 1233-47.
5. Bujnicki, J. M.; Feder, M.; Radlinska, M.; Blumenthal, R. M., Structure prediction and phylogenetic analysis of a functionally diverse family of proteins homologous to the MT-A70 subunit of the human mRNA:m(6)A methyltransferase. *J Mol Evol* **2002,** 55, (4), 431-44.
6. Liu, J.; Yue, Y.; Han, D.; Wang, X.; Fu, Y.; Zhang, L.; Jia, G.; Yu, M.; Lu, Z.; Deng, X.; Dai, Q.; Chen, W.; He, C., A METTL3-METTL14 complex mediates mammalian nuclear RNA N6-adenosine methylation. *Nat Chem Biol* **2014,** 10, (2), 93-5.
7. Śledź, P.; Jinek, M., Structural insights into the molecular mechanism of the m(6)A writer complex. *Elife* **2016,** 5, e18434.
8. Wang, P.; Doxtader, K. A.; Nam, Y., Structural basis for cooperative function of Mettl3 and Mettl14 methyltransferases. *Mol Cell* **2016,** 63, (2), 306-317.
9. Wang, X.; Feng, J.; Xue, Y.; Guan, Z.; Zhang, D.; Liu, Z.; Gong, Z.; Wang, Q.; Huang, J.; Tang, C.; Zou, T.; Yin, P., Structural basis of N(6)-adenosine methylation by the METTL3-METTL14 complex. *Nature* **2016,** 534, (7608), 575-8.
10. Ping, X. L.; Sun, B. F.; Wang, L.; Xiao, W.; Yang, X.; Wang, W. J.; Adhikari, S.; Shi, Y.; Lv, Y.; Chen, Y. S.; Zhao, X.; Li, A.; Yang, Y.; Dahal, U.; Lou, X. M.; Liu, X.; Huang, J.; Yuan, W. P.; Zhu, X. F.; Cheng, T.; Zhao, Y. L.; Wang, X.; Rendtlew Danielsen, J. M.; Liu, F.; Yang, Y. G., Mammalian WTAP is a regulatory subunit of the RNA N6-methyladenosine methyltransferase. *Cell Res* **2014,** 24, (2), 177-89.
11. Zhong, S.; Li, H.; Bodi, Z.; Button, J.; Vespa, L.; Herzog, M.; Fray, R. G., MTA is an Arabidopsis messenger RNA adenosine methylase and interacts with a homolog of a sex-specific splicing factor. *Plant Cell* **2008,** 20, (5), 1278-88.
12. Lu, L.; Zhang, Y.; He, Q.; Qi, Z.; Zhang, G.; Xu, W.; Yi, T.; Wu, G.; Li, R., MTA, an RNA m(6)A methyltransferase, enhances drought tolerance by regulating the development of trichomes and roots in poplar. *Int J Mol Sci* **2020,** 21, (7), 2462.
13. Arribas-Hernandez, L.; Bressendorff, S.; Hansen, M. H.; Poulsen, C.; Erdmann, S.; Brodersen, P., An m(6)A-YTH module controls developmental timing and morphogenesis in Arabidopsis. *Plant Cell* **2018,** 30, (5), 952-967.
14. He, Y.; Li, Y.; Yao, Y.; Zhang, H.; Wang, Y.; Gao, J.; Fan, M., Overexpression of watermelon m6A methyltransferase ClMTB enhances drought tolerance in tobacco by mitigating oxidative stress and photosynthesis inhibition and modulating stress-responsive gene expression. *Plant Physiol Bioch* **2021,** 168, 340-352.
15. Wendel, F. J.; Grover, C., *Taxonomy and evolution of the cotton genus, Gossypium*. 2nd. ed.; American Society of Agronomy Inc., Crop Science Society of America Inc., and Soil Science Society of America Inc., Madison: 2015.
16. Wang, K.; Wendel, J. F.; Hua, J., Designations for individual genomes and chromosomes in Gossypium. *Journal of Cotton Research* **2018,** 1, (1), 3.
17. Chen, Z.; Grover, C. E.; Li, P.; Wang, Y.; Nie, H.; Zhao, Y.; Wang, M.; Liu, F.; Zhou, Z.; Wang, X.; Cai, X.; Wang, K.; Wendel, J. F.; Hua, J., Molecular evolution of the plastid genome during diversification of the cotton genus. *Mol Phylogenet Evol* **2017,** 112, 268-276.
18. Huang, G.; Huang, J. Q.; Chen, X. Y.; Zhu, Y. X., Recent Advances and Future Perspectives in Cotton Research. *Annu Rev Plant Biol* **2021,** 72, 437-462.
19. Paterson, A. H.; Wendel, J. F.; Gundlach, H.; Guo, H.; Jenkins, J.; Jin, D.; Llewellyn, D.; Showmaker, K. C.; Shu, S.; Udall, J.; Yoo, M. J.; Byers, R.; Chen, W.; Doron-Faigenboim, A.; Duke, M. V.; Gong, L.; Grimwood, J.; Grover, C.; Grupp, K.; Hu, G.; Lee, T. H.; Li, J.; Lin, L.; Liu, T.; Marler, B. S.; Page, J. T.; Roberts, A. W.; Romanel, E.; Sanders, W. S.; Szadkowski, E.; Tan, X.; Tang, H.; Xu, C.; Wang, J.; Wang, Z.; Zhang, D.; Zhang, L.; Ashrafi, H.; Bedon, F.; Bowers, J. E.; Brubaker, C. L.; Chee, P. W.; Das, S.; Gingle, A. R.; Haigler, C. H.; Harker, D.; Hoffmann, L. V.; Hovav, R.; Jones, D. C.; Lemke, C.; Mansoor, S.; ur Rahman, M.; Rainville, L. N.; Rambani, A.; Reddy, U. K.; Rong, J. K.; Saranga, Y.; Scheffler, B. E.; Scheffler, J. A.; Stelly, D.

M.; Triplett, B. A.; Van Deynze, A.; Vaslin, M. F.; Waghmare, V. N.; Walford, S. A.; Wright, R. J.; Zaki, E. A.; Zhang, T.; Dennis, E. S.; Mayer, K. F.; Peterson, D. G.; Rokhsar, D. S.; Wang, X.; Schmutz, J., Repeated polyploidization of Gossypium genomes and the evolution of spinnable cotton fibres. *Nature* **2012,** 492, (7429), 423-7.

20. Wang, K.; Wang, Z.; Li, F.; Ye, W.; Wang, J.; Song, G.; Yue, Z.; Cong, L.; Shang, H.; Zhu, S.; Zou, C.; Li, Q.; Yuan, Y.; Lu, C.; Wei, H.; Gou, C.; Zheng, Z.; Yin, Y.; Zhang, X.; Liu, K.; Wang, B.; Song, C.; Shi, N.; Kohel, R. J.; Percy, R. G.; Yu, J. Z.; Zhu, Y. X.; Wang, J.; Yu, S., The draft genome of a diploid cotton Gossypium raimondii. *Nat Genet* **2012,** 44, (10), 1098-103.
21. Udall, J. A.; Long, E.; Hanson, C.; Yuan, D.; Ramaraj, T.; Conover, J. L.; Gong, L.; Arick, M. A.; Grover, C. E.; Peterson, D. G.; Wendel, J. F., De novo genome sequence assemblies of *Gossypium raimondii* and *Gossypium turneri*. *G3 (Bethesda)* **2019,** 9, (10), 3079-3085.
22. Grover, C. E.; Arick, M. A., II; Thrash, A.; Conover, J. L.; Sanders, W. S.; Peterson, D. G.; Frelichowski, J. E.; Scheffler, J. A.; Scheffler, B. E.; Wendel, J. F., Insights into the evolution of the New World diploid cottons (*Gossypium*, Subgenus Houzingenia) based on genome sequencing. *Genome Biol Evol* **2018,** 11, (1), 53-71.
23. Li, F.; Fan, G.; Wang, K.; Sun, F.; Yuan, Y.; Song, G.; Li, Q.; Ma, Z.; Lu, C.; Zou, C.; Chen, W.; Liang, X.; Shang, H.; Liu, W.; Shi, C.; Xiao, G.; Gou, C.; Ye, W.; Xu, X.; Zhang, X.; Wei, H.; Li, Z.; Zhang, G.; Wang, J.; Liu, K.; Kohel, R. J.; Percy, R. G.; Yu, J. Z.; Zhu, Y. X.; Wang, J.; Yu, S., Genome sequence of the cultivated cotton Gossypium arboreum. *Nat Genet* **2014,** 46, (6), 567-72.
24. Du, X.; Huang, G.; He, S.; Yang, Z.; Sun, G.; Ma, X.; Li, N.; Zhang, X.; Sun, J.; Liu, M.; Jia, Y.; Pan, Z.; Gong, W.; Liu, Z.; Zhu, H.; Ma, L.; Liu, F.; Yang, D.; Wang, F.; Fan, W.; Gong, Q.; Peng, Z.; Wang, L.; Wang, X.; Xu, S.; Shang, H.; Lu, C.; Zheng, H.; Huang, S.; Lin, T.; Zhu, Y.; Li, F., Resequencing of 243 diploid cotton accessions based on an updated A genome identifies the genetic basis of key agronomic traits. *Nat Genet* **2018,** 50, (6), 796-802.
25. Huang, G.; Wu, Z.; Percy, R. G.; Bai, M.; Li, Y.; Frelichowski, J. E.; Hu, J.; Wang, K.; Yu, J. Z.; Zhu, Y., Genome sequence of Gossypium herbaceum and genome updates of Gossypium arboreum and Gossypium hirsutum provide insights into cotton A-genome evolution. *Nat Genet* **2020,** 52, (5), 516-524.
26. Grover, C. E.; Pan, M.; Yuan, D.; Arick, M. A.; Hu, G.; Brase, L.; Stelly, D. M.; Lu, Z.; Schmitz, R. J.; Peterson, D. G., The *Gossypium longicalyx* genome as a resource for cotton breeding and evolution. *G3* **2020,** 10, (5), 1457-1467.
27. Cai, Y.; Cai, X.; Wang, Q.; Wang, P.; Zhang, Y.; Cai, C.; Xu, Y.; Wang, K.; Zhou, Z.; Wang, C.; Geng, S.; Li, B.; Dong, Q.; Hou, Y.; Wang, H.; Ai, P.; Liu, Z.; Yi, F.; Sun, M.; An, G.; Cheng, J.; Zhang, Y.; Shi, Q.; Xie, Y.; Shi, X.; Chang, Y.; Huang, F.; Chen, Y.; Hong, S.; Mi, L.; Sun, Q.; Zhang, L.; Zhou, B.; Peng, R.; Zhang, X.; Liu, F., Genome sequencing of the Australian wild diploid species Gossypium australe highlights disease resistance and delayed gland morphogenesis. *Plant Biotechnol J* **2020,** 18, (3), 814-828.
28. Zhang, T.; Hu, Y.; Jiang, W.; Fang, L.; Guan, X.; Chen, J.; Zhang, J.; Saski, C. A.; Scheffler, B. E.; Stelly, D. M.; Hulse-Kemp, A. M.; Wan, Q.; Liu, B.; Liu, C.; Wang, S.; Pan, M.; Wang, Y.; Wang, D.; Ye, W.; Chang, L.; Zhang, W.; Song, Q.; Kirkbride, R. C.; Chen, X.; Dennis, E.; Llewellyn, D. J.; Peterson, D. G.; Thaxton, P.; Jones, D. C.; Wang, Q.; Xu, X.; Zhang, H.; Wu, H.; Zhou, L.; Mei, G.; Chen, S.; Tian, Y.; Xiang, D.; Li, X.; Ding, J.; Zuo, Q.; Tao, L.; Liu, Y.; Li, J.; Lin, Y.; Hui, Y.; Cao, Z.; Cai, C.; Zhu, X.; Jiang, Z.; Zhou, B.; Guo, W.; Li, R.; Chen, Z. J., Sequencing of allotetraploid cotton (Gossypium hirsutum L. acc. TM-1) provides a resource for fiber improvement. *Nat Biotechnol* **2015,** 33, (5), 531-7.
29. Chen, Z. J.; Sreedasyam, A.; Ando, A.; Song, Q.; De Santiago, L. M.; Hulse-Kemp, A. M.; Ding, M.; Ye, W.; Kirkbride, R. C.; Jenkins, J.; Plott, C.; Lovell, J.; Lin, Y. M.; Vaughn, R.; Liu, B.; Simpson, S.; Scheffler, B. E.; Wen, L.; Saski, C. A.; Grover, C. E.; Hu, G.; Conover, J. L.; Carlson, J. W.; Shu, S.; Boston, L. B.; Williams, M.; Peterson, D. G.; McGee, K.; Jones, D. C.; Wendel, J. F.; Stelly, D. M.; Grimwood, J.; Schmutz, J., Genomic diversifications of five Gossypium allopolyploid species and their impact on cotton improvement. *Nat Genet* **2020,** 52, (5), 525-533.

30. Li, F.; Fan, G.; Lu, C.; Xiao, G.; Zou, C.; Kohel, R. J.; Ma, Z.; Shang, H.; Ma, X.; Wu, J.; Liang, X.; Huang, G.; Percy, R. G.; Liu, K.; Yang, W.; Chen, W.; Du, X.; Shi, C.; Yuan, Y.; Ye, W.; Liu, X.; Zhang, X.; Liu, W.; Wei, H.; Wei, S.; Zhu, S.; Zhang, H.; Sun, F.; Wang, X.; Liang, J.; Wang, J.; He, Q.; Huang, L.; Cui, J.; Song, G.; Wang, K.; Xu, X.; Yu, J. Z.; Zhu, Y.; Yu, S., Genome sequence of cultivated Upland cotton (Gossypium hirsutum TM-1) provides insights into genome evolution. *Nat Biotechnol* **2015,** 33, (5), 524-30.
31. Liu, X.; Zhao, B.; Zheng, H. J.; Hu, Y.; Lu, G.; Yang, C. Q.; Chen, J. D.; Chen, J. J.; Chen, D. Y.; Zhang, L.; Zhou, Y.; Wang, L. J.; Guo, W. Z.; Bai, Y. L.; Ruan, J. X.; Shangguan, X. X.; Mao, Y. B.; Shan, C. M.; Jiang, J. P.; Zhu, Y. Q.; Jin, L.; Kang, H.; Chen, S. T.; He, X. L.; Wang, R.; Wang, Y. Z.; Chen, J.; Wang, L. J.; Yu, S. T.; Wang, B. Y.; Wei, J.; Song, S. C.; Lu, X. Y.; Gao, Z. C.; Gu, W. Y.; Deng, X.; Ma, D.; Wang, S.; Liang, W. H.; Fang, L.; Cai, C. P.; Zhu, X. F.; Zhou, B. L.; Jeffrey Chen, Z.; Xu, S. H.; Zhang, Y. G.; Wang, S. Y.; Zhang, T. Z.; Zhao, G. P.; Chen, X. Y., Gossypium barbadense genome sequence provides insight into the evolution of extra-long staple fiber and specialized metabolites. *Sci Rep* **2015,** 5, 14139.
32. Yuan, D.; Tang, Z.; Wang, M.; Gao, W.; Tu, L.; Jin, X.; Chen, L.; He, Y.; Zhang, L.; Zhu, L.; Li, Y.; Liang, Q.; Lin, Z.; Yang, X.; Liu, N.; Jin, S.; Lei, Y.; Ding, Y.; Li, G.; Ruan, X.; Ruan, Y.; Zhang, X., The genome sequence of Sea-Island cotton (Gossypium barbadense) provides insights into the allopolyploidization and development of superior spinnable fibres. *Sci Rep* **2015,** 5, 17662.
33. Wang, M.; Tu, L.; Yuan, D.; Zhu; Shen, C.; Li, J.; Liu, F.; Pei, L.; Wang, P.; Zhao, G.; Ye, Z.; Huang, H.; Yan, F.; Ma, Y.; Zhang, L.; Liu, M.; You, J.; Yang, Y.; Liu, Z.; Huang, F.; Li, B.; Qiu, P.; Zhang, Q.; Zhu, L.; Jin, S.; Yang, X.; Min, L.; Li, G.; Chen, L. L.; Zheng, H.; Lindsey, K.; Lin, Z.; Udall, J. A.; Zhang, X., Reference genome sequences of two cultivated allotetraploid cottons, Gossypium hirsutum and Gossypium barbadense. *Nat Genet* **2019,** 51, (2), 224-229.
34. Hu, Y.; Chen, J.; Fang, L.; Zhang, Z.; Ma, W.; Niu, Y.; Ju, L.; Deng, J.; Zhao, T.; Lian, J.; Baruch, K.; Fang, D.; Liu, X.; Ruan, Y. L.; Rahman, M. U.; Han, J.; Wang, K.; Wang, Q.; Wu, H.; Mei, G.; Zang, Y.; Han, Z.; Xu, C.; Shen, W.; Yang, D.; Si, Z.; Dai, F.; Zou, L.; Huang, F.; Bai, Y.; Zhang, Y.; Brodt, A.; Ben-Hamo, H.; Zhu, X.; Zhou, B.; Guan, X.; Zhu, S.; Chen, X.; Zhang, T., Gossypium barbadense and Gossypium hirsutum genomes provide insights into the origin and evolution of allotetraploid cotton. *Nat Genet* **2019,** 51, (4), 739-748.
35. Yang, Z.; Ge, X.; Yang, Z.; Qin, W.; Sun, G.; Wang, Z.; Li, Z.; Liu, J.; Wu, J.; Wang, Y.; Lu, L.; Wang, P.; Mo, H.; Zhang, X.; Li, F., Extensive intraspecific gene order and gene structural variations in upland cotton cultivars. *Nat Commun* **2019,** 10, (1), 2989.
36. Udall, J. A.; Long, E.; Ramaraj, T.; Conover, J. L.; Yuan, D.; Grover, C. E.; Gong, L.; Arick, M. A., 2nd; Masonbrink, R. E.; Peterson, D. G.; Wendel, J. F., The genome sequence of *Gossypioides kirkii* illustrates a descending dysploidy in plants. *Front Plant Sci* **2019,** 10, 1541.
37. Liu, J.; Li, K.; Cai, J.; Zhang, M.; Zhang, X.; Xiong, X.; Meng, H.; Xu, X.; Huang, Z.; Peng, J.; Fan, J.; Yi, C., Landscape and Regulation of m(6)A and m(6)Am Methylome across Human and Mouse Tissues. *Mol Cell* **2020,** 77, (2), 426-440 e6.
38. Hernandez-Garcia, C. M.; Finer, J. J., Identification and validation of promoters and cis-acting regulatory elements. *Plant Sci* **2014,** 217-218, 109-19.
39. Lescot, M.; Dehais, P.; Thijs, G.; Marchal, K.; Moreau, Y.; Van de Peer, Y.; Rouze, P.; Rombauts, S., PlantCARE, a database of plant cis-acting regulatory elements and a portal to tools for in silico analysis of promoter sequences. *Nucleic Acids Res* **2002,** 30, (1), 325-7.
40. Wang, X.; Lu, Z.; Gomez, A.; Hon, G. C.; Yue, Y.; Han, D.; Fu, Y.; Parisien, M.; Dai, Q.; Jia, G.; Ren, B.; Pan, T.; He, C., N6-methyladenosine-dependent regulation of messenger RNA stability. *Nature* **2014,** 505, (7481), 117-20.
41. Zhao, X.; Yang, Y.; Sun, B. F.; Shi, Y.; Yang, X.; Xiao, W.; Hao, Y. J.; Ping, X. L.; Chen, Y. S.; Wang, W. J.; Jin, K. X.; Wang, X.; Huang, C. M.; Fu, Y.; Ge, X. M.; Song, S. H.; Jeong, H. S.; Yanagisawa, H.; Niu, Y.; Jia, G. F.; Wu, W.; Tong, W. M.; Okamoto,

A.; He, C.; Rendtlew Danielsen, J. M.; Wang, X. J.; Yang, Y. G., FTO-dependent demethylation of N6-methyladenosine regulates mRNA splicing and is required for adipogenesis. *Cell Res* **2014,** 24, (12), 1403-19.

42. Shi, H.; Wang, X.; Lu, Z.; Zhao, B. S.; Ma, H.; Hsu, P. J.; Liu, C.; He, C., YTHDF3 facilitates translation and decay of N(6)-methyladenosine-modified RNA. *Cell Res* **2017,** 27, (3), 315-328.
43. Visvanathan, A.; Somasundaram, K., mRNA traffic control reviewed: N6-methyladenosine (m(6) A) takes the driver's seat. *Bioessays* **2018,** 40, (1), 1700093.
44. Bodi, Z.; Zhong, S.; Mehra, S.; Song, J.; Li, H.; Graham, N.; May, S.; Fray, R., Adenosine methylation in Arabidopsis mRNA is associated with the 3′ end and reduced levels cause developmental defects. *Front Plant Sci* **2012,** 3, 48.
45. Růžička, K.; Zhang, M.; Campilho, A.; Bodi, Z.; Kashif, M.; Saleh, M.; Eeckhout, D.; El-Showk, S.; Li, H.; Zhong, S.; De Jaeger, G.; Mongan, N. P.; Hejátko, J.; Helariutta, Y.; Fray, R. G., Identification of factors required for m6A mRNA methylation in Arabidopsis reveals a role for the conserved E3 ubiquitin ligase HAKAI. *New Phytol* **2017,** 215, (1), 157-172.
46. Zhang, F.; Zhang, Y. C.; Liao, J. Y.; Yu, Y.; Zhou, Y. F.; Feng, Y. Z.; Yang, Y. W.; Lei, M. Q.; Bai, M.; Wu, H.; Chen, Y. Q., The subunit of RNA N6-methyladenosine methyltransferase OsFIP regulates early degeneration of microspores in rice. *PLoS Genet* **2019,** 15, (5), e1008120.
47. Sharma, P.; Chatterjee, M.; Burman, N.; Khurana, J. P., Cryptochrome 1 regulates growth and development in Brassica through alteration in the expression of genes involved in light, phytohormone and stress signalling. *Plant Cell Environ* **2014,** 37, (4), 961-77.
48. Lopez, L.; Carbone, F.; Bianco, L.; Giuliano, G.; Facella, P.; Perrotta, G., Tomato plants overexpressing cryptochrome 2 reveal altered expression of energy and stress-related gene products in response to diurnal cues. *Plant Cell Environ* **2012,** 35, (5), 994-1012.
49. D'Amico-Damiao, V.; Carvalho, R. F., Cryptochrome-Related Abiotic Stress Responses in Plants. *Front Plant Sci* **2018,** 9, 1897.
50. D'Amico-Damiao, V.; Lucio, J. C. B.; Oliveira, R.; Gaion, L. A.; Barreto, R. F.; Carvalho, R. F., Cryptochrome 1a depends on blue light fluence rate to mediate osmotic stress responses in tomato. *J Plant Physiol* **2021,** 258-259, 153374.
51. Meyer, K. D.; Patil, D. P.; Zhou, J.; Zinoviev, A.; Skabkin, M. A.; Elemento, O.; Pestova, T. V.; Qian, S. B.; Jaffrey, S. R., 5' UTR m(6)A Promotes Cap-Independent Translation. *Cell* **2015,** 163, (4), 999-1010.
52. Hu, J.; Cai, J.; Park, S. J.; Lee, K.; Li, Y.; Chen, Y.; Yun, J. Y.; Xu, T.; Kang, H., N(6) -Methyladenosine mRNA methylation is important for salt stress tolerance in Arabidopsis. *Plant J* **2021,** 106, (6), 1759-1775.
53. Li, Z.; Shi, J.; Yu, L.; Zhao, X.; Ran, L.; Hu, D.; Song, B., N (6) -methyl-adenosine level in Nicotiana tabacum is associated with tobacco mosaic virus. *Virol J* **2018,** 15, (1), 87.
54. Miao, Z.; Zhang, T.; Qi, Y.; Song, J.; Han, Z.; Ma, C., Evolution of the RNA N (6)-Methyladenosine Methylome Mediated by Genomic Duplication. *Plant Physiol* **2020,** 182, (1), 345-360.
55. Wendel, J. F., The wondrous cycles of polyploidy in plants. *Am J Bot* **2015,** 102, (11), 1753-6.
56. Chen, Z.; Cao, J. B.; Zhang, X.; Shangguan, X.; Mao, Y.-B.; Wang, L.-J.; Chen, X.-Y., Cotton genome: challenge into the polyploidy. *Chinese Science Bulletin* **2017,** 62, 1622-1623.
57. Meyer, Kate D.; Saletore, Y.; Zumbo, P.; Elemento, O.; Mason, Christopher E.; Jaffrey, Samie R., Comprehensive Analysis of mRNA Methylation Reveals Enrichment in 3′ UTRs and near Stop Codons. *Cell* **2012,** 149, (7), 1635-1646.
58. Meyer, K. D.; Jaffrey, S. R., Rethinking m(6)A readers, writers, and erasers. *Annu Rev Cell Dev Biol* **2017,** 33, 319-342.
59. Luo, G. Z.; MacQueen, A.; Zheng, G.; Duan, H.; Dore, L. C.; Lu, Z.; Liu, J.; Chen, K.; Jia, G.; Bergelson, J.; He, C., Unique features of the m6A methylome in Arabidopsis thaliana. *Nat Commun* **2014,** 5, 5630.
60. Yu, J.; Jung, S.; Cheng, C. H.; Ficklin, S. P.; Lee, T.; Zheng, P.; Jones, D.; Percy, R. G.; Main, D., CottonGen: a genomics, genetics and breeding database for cotton research. *Nucleic acids research* **2014,** 42, (Database issue), 1229-36.

61. Wong, D. C.; Schlechter, R.; Vannozzi, A.; Holl, J.; Hmmam, I.; Bogs, J.; Tornielli, G. B.; Castellarin, S. D.; Matus, J. T., A systems-oriented analysis of the grapevine R2R3-MYB transcription factor family uncovers new insights into the regulation of stilbene accumulation. *DNA Res* **2016**.
62. Mistry, J.; Finn, R. D.; Eddy, S. R.; Bateman, A.; Punta, M., Challenges in homology search: HMMER3 and convergent evolution of coiled-coil regions. *Nucleic Acids Res* **2013,** 41, (12), e121.
63. Finn, R. D.; Mistry, J.; Schuster-Bockler, B.; Griffiths-Jones, S.; Hollich, V.; Lassmann, T.; Moxon, S.; Marshall, M.; Khanna, A.; Durbin, R.; Eddy, S. R.; Sonnhammer, E. L.; Bateman, A., Pfam: clans, web tools and services. *Nucleic Acids Res* **2006,** 34, (Database issue), D247-51.
64. Wheeler, T. J.; Eddy, S. R., nhmmer: DNA homology search with profile HMMs. *Bioinformatics* **2013,** 29, (19), 2487-9.
65. Poole, R. L., The TAIR database. *Methods in molecular biology* **2007,** 406, 179-212.
66. Letunic, I.; Bork, P., 20 years of the SMART protein domain annotation resource. *Nucleic acids research* **2018,** 46, (D1), D493-D496.
67. Finn, R. D.; Coggill, P.; Eberhardt, R. Y.; Eddy, S. R.; Mistry, J.; Mitchell, A. L.; Potter, S. C.; Punta, M.; Qureshi, M.; Sangrador-Vegas, A.; Salazar, G. A.; Tate, J.; Bateman, A., The Pfam protein families database: towards a more sustainable future. *Nucleic Acids Res* **2016,** 44, (D1), D279-85.
68. Chen, C.; Chen, H.; Zhang, Y.; Thomas, H. R.; Frank, M. H.; He, Y.; Xia, R., TBtools: An Integrative Toolkit Developed for Interactive Analyses of Big Biological Data. *Mol Plant* **2020,** 13, (8), 1194-1202.
69. Hu, B.; Jin, J.; Guo, A. Y.; Zhang, H.; Luo, J.; Gao, G., GSDS 2.0: an upgraded gene feature visualization server. *Bioinformatics* **2015,** 31, (8), 1296-7.
70. Wilkins, M. R.; Gasteiger, E.; Bairoch, A.; Sanchez, J. C.; Williams, K. L.; Appel, R. D.; Hochstrasser, D. F., Protein identification and analysis tools in the ExPASy server. *Methods in molecular biology* **1999,** 112, 531-52.
71. Katoh, K.; Standley, D. M., MAFFT multiple sequence alignment software version 7: improvements in performance and usability. *Molecular Biology & Evolution* **2013,** 30, (4), 772.
72. Tamura, K.; Stecher, G.; Peterson, D.; Filipski, A.; Kumar, S., MEGA6: Molecular Evolutionary Genetics Analysis version 6.0. *Mol Biol Evol* **2013,** 30, (12), 2725-9.
73. Zhao, B.; Cao, J. F.; Hu, G. J.; Chen, Z. W.; Wang, L. Y.; Shangguan, X. X.; Wang, L. J.; Mao, Y. B.; Zhang, T. Z.; Wendel, J. F.; Chen, X. Y., Core cis-element variation confers subgenome-biased expression of a transcription factor that functions in cotton fiber elongation. *New Phytol* **2018,** 218, (3), 1061-1075.
74. Kim, D.; Langmead, B.; Salzberg, S. L., HISAT: a fast spliced aligner with low memory requirements. *Nat Methods* **2015,** 12, (4), 357-60.
75. Pertea, M.; Kim, D.; Pertea, G. M.; Leek, J. T.; Salzberg, S. L., Transcript-level expression analysis of RNA-seq experiments with HISAT, StringTie and Ballgown. *Nat Protoc* **2016,** 11, (9), 1650-67.
76. Risso, D.; Ngai, J.; Speed, T. P.; Dudoit, S., Normalization of RNA-seq data using factor analysis of control genes or samples. *Nat Biotechnol* **2014,** 32, (9), 896-902.
77. Wang, M.; Wang, Q.; Zhang, B., Evaluation and selection of reliable reference genes for gene expression under abiotic stress in cotton (*Gossypium hirsutum* L.). *Gene* **2013,** 530, (1), 44-50.
78. Zhang, Y.; Parmigiani, G.; Johnson, W. E., Combat-seq: batch effect adjustment for RNA-seq count data. *bioRxiv* **2020**, 2020.01.13.904730.
79. You, Q.; Xu, W. Y.; Zhang, K.; Zhang, L. W.; Yi, X.; Yao, D. X.; Wang, C. C.; Zhang, X. Y.; Zhao, X. H.; Provart, N. J.; Li, F. G.; Su, Z., ccNET: Database of co-expression networks with functional modules for diploid and polyploid *Gossypium*. *Nucleic acids research* **2017,** 45, (9), 5625-5626.

80. Huang, C.; Li, P.; Cao, J.; Zheng, Z.; Huang, J.; Zhang, X.; Shangguan, X.; Wang, L.; Chen, Z., Comprehensive identification and expression analysis of CRY gene family in Gossypium. *BMC Genomics* **2022,** 23, (1), 231.
81. Zhu, J.; Chen, J.; Gao, F.; Xu, C.; Wu, H.; Chen, K.; Si, Z.; Yan, H.; Zhang, T., Rapid mapping and cloning of the virescent-1 gene in cotton by bulked segregant analysis-next generation sequencing and virus-induced gene silencing strategies. *J Exp Bot* **2017,** 68, (15), 4125-4135.
82. Tian, X.; Ruan, J. X.; Huang, J. Q.; Yang, C. Q.; Fang, X.; Chen, Z. W.; Hong, H.; Wang, L. J.; Mao, Y. B.; Lu, S.; Zhang, T. Z.; Chen, X. Y., Characterization of gossypol biosynthetic pathway. *Proc Natl Acad Sci U S A* **2018,** 115, (23), E5410-E5418.
83. Huang, J. Q.; Fang, X.; Tian, X.; Chen, P.; Lin, J. L.; Guo, X. X.; Li, J. X.; Fan, Z.; Song, W. M.; Chen, F. Y.; Ahati, R.; Wang, L. J.; Zhao, Q.; Martin, C.; Chen, X. Y., Aromatization of natural products by a specialized detoxification enzyme. *Nat Chem Biol* **2020,** 16, (3), 250-256.
84. Cao, J.-F.; Huang, J.-Q.; Liu, X.; Huang, C.-C.; Zheng, Z.-S.; Zhang, X.-F.; Shangguan, X.-X.; Wang, L.-J.; Zhang, Y.-G.; Wendel, J. F.; Grover, C. E.; Chen, Z.-W., Genome-wide characterization of the GRF family and their roles in response to salt stress in Gossypium. *BMC Genomics* **2020,** 21, (1), 575.
85. Zhang, X.; Cao, J.; Huang, C.; Zheng, Z.; Liu, X.; Shangguan, X.; Wang, L.; Zhang, Y.; Chen, Z., Characterization of cotton ARF factors and the role of GhARF2b in fiber development. *BMC Genomics* **2021,** 22, (1), 202.
86. Cui, W.; Chen, Z.; Shangguan, X.; Li, T.; Wang, L.; Xue, X.; Cao, J., TRY intron2 determined its expression in inflorescence activated by SPL9 and MADS-box genes in Arabidopsis. *Plant Sci* **2022,** 321, 111311.
87. Livak, K. J.; Schmittgen, T. D., Analysis of relative gene expression data using real-time quantitative PCR and the 2(T)(-Delta Delta C) method. *Methods* **2001,** 25, (4), 402-408.
88. Liu, J. e.; Li, K.; Cai, J.; Zhang, M.; Zhang, X.; Xiong, X.; Meng, H.; Xu, X.; Huang, Z.; Peng, J.; Fan, J.; Yi, C., Landscape and regulation of m^6A and m^6Am methylome across human and mouse tissues. *Mol Cell* **2020,** 77, (2), 426-440.e6.
89. Cao, J. F.; Zhao, B.; Huang, C. C.; Chen, Z. W.; Zhao, T.; Liu, H. R.; Hu, G. J.; Shangguan, X. X.; Shan, C. M.; Wang, L. J.; Zhang, T. Z.; Wendel, J. F.; Guan, X. Y.; Chen, X. Y., The miR319-Targeted GhTCP4 Promotes the Transition from Cell Elongation to Wall Thickening in Cotton Fiber. *Mol Plant* **2020,** 13, (7), 1063-1077.
90. Bent, A., Arabidopsis thaliana floral dip transformation method. *Methods Mol Biol* **2006,** 343, 87-103.
91. Shangguan, X.; Yang, Q.; Wu, X.; Cao, J., Function analysis of a cotton R2R3 MYB transcription factor GhMYB3 in regulating plant trichome development. *Plant Biol (Stuttg)* **2021,** 23, (6), 1118-1127.
92. Chen, Z.; Zhao, J.; Song, J.; Han, S.; Du, Y.; Qiao, Y.; Liu, Z.; Qiao, J.; Li, W.; Li, J.; Wang, H.; Xing, B.; Pan, Q., Influence of graphene on the multiple metabolic pathways of Zea mays roots based on transcriptome analysis. *PloS ONE* **2021,** 16, (1), e0244856.
93. Chen, Z.; Zhao, J.; Qiao, J.; Li, W.; Guan, Z.; Liu, Z.; Bai, X.; Xing, B.; Zhang, J.; Li, J.; Yin, W.; Zhu, H., Graphene-mediated antioxidant enzyme activity and respiration in plant roots. *ACS Agricultural Science & Technology* **2022,** 2, (3), 646-660.
94. Love, M. I.; Huber, W.; Anders, S., Moderated estimation of fold change and dispersion for RNA-seq data with DESeq2. *Genome Biol* **2014,** 15, (12), 550.
95. Mao, X.; Cai, T.; Olyarchuk, J. G.; Wei, L., Automated genome annotation and pathway identification using the KEGG Orthology (KO) as a controlled vocabulary. *Bioinformatics* **2005,** 21, (19), 3787-3793.